water

MDPI

Article

Efficient Removal of Ammonium Nitrogen from Aquatic Systems Using Thermally and Alkali-Modified Diatomite and Zeolite

Gulfairus Bizhanova [1], Maral Abdibattayeva [1], Wang Ping [2], Umut Mussina [3], Laura Kurbanova [1], Arman Zhumazhanov [1,4], Dana Akhmetzhanova [1,4], Ospan Doszhanov [5], Bekzat Ismukhanbetov [5], Didar Bolatova [4,6] and Yerlan Doszhanov [1,4,*]

1 UNESCO Chair in Sustainable Development, Al-Farabi Kazakh National University, Al-Farabi Ave. 71, Almaty 050040, Kazakhstan; gulfairus82@mail.ru (G.B.); abdybattaeva.maral@kaznu.kz (M.A.); kurbanova.l.2025@mail.ru (L.K.); jumajanarman@gmail.com (A.Z.); adana128128@gmail.com (D.A.)
2 Institute of Geographic Sciences and Natural Resources Research, Chinese Academy of Sciences, 11A, Datun Road, Chaoyang District, Beijing 100101, China; wangping@igsnrr.ac.cn
3 LLP Scientific Diagnostic Center "Animal Expert Group", St. Magnetnaya, 19B, Almaty 050054, Kazakhstan; 07061960@mail.ru
4 Institute of Combustion Problems, Bogenbay Batyr Str., 172, Almaty 050012, Kazakhstan; dikobolatova.db@gmail.com
5 Faculty of Engineering and Information Technology, Almaty Technological University, Tole Bi Str., 100, Almaty 050061, Kazakhstan; ospan.doszhanov@mail.ru (O.D.); beka6768@gmail.com (B.I.)
6 Department of Science, International IT University, Manas 34/1, Almaty 050040, Kazakhstan
* Correspondence: yerlan.doszhanov@kaznu.edu.kz

Abstract

Ammonium nitrogen (NH_4^+-N) is a key biogenic pollutant in aquatic systems. This study evaluated natural diatomite (Aktobe region) and zeolite (Shankhanai, Zhetysu region) as low-cost, environmentally benign sorbents for NH_4^+-N removal, and examined the effects of thermal (200–750 °C; 450 °C selected) and alkaline (0.5 M NaOH) treatments on their structural, textural and adsorption properties. Materials were characterized by XRD, XRF, FTIR, SEM-EDX and adsorption performance was assessed by kinetic and equilibrium experiments. Specific surface area and pore characteristics were determined from low-temperature nitrogen adsorption–desorption measurements, and the specific surface area was calculated using the Brunauer–Emmett–Teller (BET) method. Thermal treatment at 450 °C increased the specific surface area of diatomite (46.3 m^2/g) and pore volume, and subsequent alkaline activation further enhanced adsorption activity. The modified diatomite achieved up to 84.6% removal of NH_4^+-N with an equilibrium capacity q_{max} = 1.758 mg/g. Adsorption kinetics were best described by the pseudo-second-order (PSO) model, which may indicate a substantive role of surface chemical interactions. Equilibrium data were fitted with Langmuir and Freundlich models: the modified diatomite fitted Langmuir best (R^2 = 0.999), which may suggest predominance of a monolayer adsorption mechanism under the studied conditions, whereas natural samples and the zeolite were better described by the Freundlich model, reflecting likely surface energetic heterogeneity. Separation factor values (R_L = 0.068–0.643) indicate favorable adsorption within the investigated concentration range. The point of zero charge (pHpzc) was determined for all sorbents (5.3–6.3), confirming that at pH 7 the surface carries a negative charge favorable for electrostatic attraction of NH_4^+ cations. Reusability tests over five consecutive adsorption–desorption cycles showed that modified diatomite and modified zeolite retained 93.4% and 92.3% of their initial removal efficiency, respectively, indicating acceptable stability under the applied regeneration conditions. These results demonstrate the potential of alkaline-modified diatomite and zeolite as effective sorbents for ammonium removal from wastewaters, contributing to the mitigation of eutrophication risks.

Check for updates

Academic Editor: Andrea G. Capodaglio

Received: 11 March 2026
Revised: 27 April 2026
Accepted: 1 May 2026
Published: 4 May 2026

Copyright: © 2026 by the authors. Licensee MDPI, Basel, Switzerland. This article is an open access article distributed under the terms and conditions of the Creative Commons Attribution (CC BY) license.

Keywords: natural sorbents; ammonium nitrogen; thermal modification; alkaline modification; water purification; aquatic ecosystems; sorption kinetics; eutrophication; diatomite; zeolite

1. Introduction

Pollution of water bodies by wastewater from livestock complexes (manure, liquid waste from sheep and cattle farming), municipal wastewater, as well as industrial emissions (food, chemical, pharmaceutical, coke-chemical and fertilizer industries) is a serious environmental problem in many countries. The influx of biogenic elements, primarily nitrogen and phosphorus compounds, leads to disruption of the trophic balance of reservoirs, the development of eutrophication, intense algal blooms, a decrease in dissolved oxygen concentration, death of aquatic organisms and deterioration of drinking water quality [1–3].

Ammonium nitrogen (NH_4^+-N) is one of the main pollutants of the aquatic environment, since it is formed during the decomposition of organic substances, has high mobility in the aqueous phase and, when oxidized to nitrites and nitrates, can enhance the processes of secondary pollution and toxicity [4]. In aqueous systems, ammonium nitrogen (NH_4^+-N) is present in the form of ammonium ions (NH_4^+). While NH_4^+ refers to the chemical species in solution, NH_4^+-N denotes the nitrogen content associated with this form and is commonly used in environmental and analytical assessments. In the present study, removal efficiency is expressed in terms of ammonium nitrogen (NH_4^+-N).

Various methods are used to remove ammonium from aqueous media, including biological nitrification-denitrification (air stripping), chemical precipitation (for example, in the form of struvite), and membrane technologies [5]. However, biological processes are sensitive to temperature and toxic loads, require significant energy consumption and long processing time; airborne desorption is effective mainly at high pH values; chemical precipitation is associated with the consumption of reagents and the formation of secondary precipitation; membrane methods are characterized by high cost and the problem of membrane contamination. In this regard, adsorption is considered as a more technologically simple, economically feasible and effective alternative, providing a high degree of ammonium nitrogen removal at relatively low operating costs [6].

The growing need for efficient and affordable treatment technologies makes the use of natural mineral sorbents particularly relevant. In many wastewater treatment applications, especially in regions with limited access to advanced infrastructure, the high cost and operational complexity of membrane, biological, or chemically intensive methods restrict their practical implementation. Under such conditions, diatomite and zeolite are attractive because they are naturally abundant, inexpensive, chemically stable, and environmentally benign materials that can be used with minimal preprocessing. Their value lies not only in their sorption potential but also in their suitability for scalable and decentralized water-treatment systems. This is especially important for countries such as Kazakhstan, where local deposits of diatomite and zeolite provide a promising basis for the development of low-cost sorbents for environmental applications.

Diatomite and zeolite are natural mineral materials that are widely considered as potentially cheap sorbents for removing ammonium forms of nitrogen from water (in the literature, this can be described as NH_4^+ or NH_4^+-N removal) [7–9]. However, the effectiveness of natural minerals is determined by their initial structure and surface chemistry, as well as the experimental conditions and associated impurities (ammonium concentration, presence of competing cations, suspended solids), so the issue of pre-directed modification of materials becomes especially important [9–13].

Diatomite can exhibit sorption activity to ammonium compounds and be used as a component of filtration plants. In the rain garden model systems, the addition of diatomite to the filter substrate led to a noticeable increase in the degree of purification from NH_4^+ compared with the control system without diatomite (a decrease in NH_4^+ concentration of the order of 93–94% was shown for laboratory columns) [8]. At the same time, the sorption capacity of natural diatomite for NH_4^+-N may be limited: in the work considering diatomite as a potential permeable reactive barrier medium, the maximum capacity was about 0.677 mg/g, which indicates the need for modification when focusing on a "purely sorption" scheme [14]. At the same time, diatomite has shown a strong ability to load and develop nitrifying communities and a high degree of sorbent bioregeneration (more than 80% under experimental conditions), which makes it promising for hybrid solutions such as "sorption + bioprocess" [14]. A significant increase in efficiency was observed during chemical functionalization and the creation of composites: the combination of H_2SO_4, NaCl, and calcination formed a diatomaceous sorbent, which provides more than 80% removal of ammonium nitrogen from model water and stability in adsorption–desorption cycles [7], and composite solutions based on diatomite and MgO/CaO demonstrated high recovery rates ammonium in batches and columns when working with natural water [15].

Zeolites are traditionally considered as more "selective" materials for ammonium due to the ion exchange mechanism and the ability to extract NH_4^+ even in the presence of competing ions [9–12,16]. Some studies emphasize that the Si/Al ratio and the cationic composition of zeolite determine the proportion of ion exchange and physical adsorption, and the dominant mechanism may change at different concentrations of NH_4^+ [16]. The practical applicability of zeolites is also related to the possibility of regeneration: salt regeneration (for example, with NaCl solutions) and conversion to the Na form make it possible to maintain high capacities and stability over multiple cycles, which is critical for the economic efficiency of the technology [12,17,18]. Moreover, modern works consider zeolite schemes not only as removal, but also as extraction of ammonium with subsequent resource use, including the production of concentrated ammonium-containing regenerates and their potential use for fertilizers [19–21].

Given the limitations of natural forms of materials, their modification is of particular importance. For diatomite, alkaline NaOH treatment is described as a way to change the morphology and surface (including the formation of additional Si-OH groups), and under the right conditions, to rebuild the porous structure and increase the specific surface area, which can increase sorption characteristics [22–24]. For zeolites, alkaline modification can also change porosity and active centers, but its effect depends on the composition of a particular mineral: NaOH can both improve and worsen adsorption properties, including cases of damage to the skeleton structure and decrease in microporosity [9,13]. For this reason, heat treatment, often used to prepare diatomite or as a functionalization element, requires caution for zeolites: the literature shows that intense heating can lead to a deterioration in the efficiency of NH_4^+-N removal due to the destruction of the crystalline framework [7,25].

Despite the considerable number of studies devoted to ammonium removal using diatomite and zeolites, sorption characteristics vary significantly depending on the type of material modification. Chemical functionalization and alkaline treatments are well documented in the literature. However, the combined effect of moderate thermal treatment and mild alkaline activation of diatomite, together with a direct comparison to zeolite modified without high thermal treatment, has been less systematically addressed. Therefore, additional analysis of the selected activation approaches is warranted for NH_4^+-N removal.

The aim of this study is to investigate the efficiency of thermally and alkali-modified diatomite and zeolite for ammonium nitrogen removal from aqueous solutions and to

evaluate the adsorption mechanisms and kinetic behavior of the process. This study investigates how moderate calcination of diatomite combined with subsequent alkaline treatment affects its ability to remove ammonium nitrogen, with parallel comparison to zeolite modified under identical alkaline conditions.

The novelty of this study lies in a systematic comparative assessment of locally sourced diatomite and zeolite from Kazakhstan under a unified mild modification strategy. Specifically, the work identifies 450 °C as the optimal thermal pretreatment temperature for diatomite, followed by 0.5 M NaOH activation, and directly compares the resulting sorption behavior with that of alkali-treated zeolite under the same chemical activation conditions. In addition, the study combines specific surface area, XRD, FTIR, SEM, ζ-potential, and DLS analyses to link structural and surface changes with ammonium removal performance. Therefore, the contribution of this work is not the demonstration of a record-high capacity, but the clarification of how low-cost modification improves locally available mineral sorbents for ammonium removal.

2. Materials and Methods

2.1. Raw Materials and Preparation of Sorbents

Natural zeolite from the Shankhanai deposit (Zhetysu Region, Kazakhstan) and natural diatomite from a deposit in the Aktobe Region, Kazakhstan, were used as raw materials.

The diatomite was mechanically milled and sieved to obtain a homogeneous particle size fraction of 0.5–2 mm. Prior to modification, the diatomite samples were dried at 105 °C to constant weight in order to remove physically adsorbed moisture. Additionally, diatomite was subjected to thermal treatment at 200, 450, 550, 650, and 750 °C for 120 min in a muffle furnace to evaluate the effect of heating on phase composition, textural characteristics, and sorption properties.

The zeolite fraction (0.5–2 mm) was heated at 150 °C for 12 h to remove physically bound water without altering the crystalline framework. The difference in thermal treatment protocols for the two minerals is dictated by their distinct structural properties. For diatomite, calcination at 450 °C is necessary to clear the porous network of organic matter and enhance surface accessibility. For the zeolite, a lower temperature (150 °C) was selected to ensure effective dehydration while preventing potential framework instability or loss of ion-exchange capacity, which can occur in crystalline aluminosilicates at higher temperatures.

Alkaline modification of diatomite and zeolite was carried out by treatment with a 0.5 M NaOH (Sigma-Aldrich, St. Louis, MO, USA) solution at room temperature under constant stirring. The solid-to-liquid ratio was 1:10 (g/mL). NaOH at a concentration of 0.5 M was selected as a moderate activating agent for modifying the sorbent surface under controlled conditions. The treatment was performed for 2 h, after which the samples were washed with distilled water until a neutral pH of the filtrate was achieved and then dried at 105 °C to constant weight.

2.2. Assessment of Structural and Chemical Characteristics

The phase composition of the raw and thermally treated diatomite samples was determined by X-ray diffraction (XRD) using a Bruker D8 Advance diffractometer (Bruker AXS, Karlsruhe, Germany) with Cu Kα radiation (λ = 1.5406 Å). Mineral phase identification was performed by comparing the experimental diffraction patterns with the PDF-2 database [26]. The analysis was qualitative in nature and was used to assess changes in the crystalline structure following thermal and alkaline modification.

The oxide composition of the raw zeolite and diatomite samples was determined by X-ray fluorescence (XRF) analysis using a Panalytical Axios spectrometer (PANalytical B.V.,

Almelo, The Netherlands) (1 kW). Quantitative contents of the major oxides (SiO_2, Al_2O_3, Fe_2O_3, CaO, MgO, K_2O, Na_2O, TiO_2, etc.) were obtained and used to interpret the influence of chemical composition on the sorption properties of the materials.

Surface functional groups were analyzed by Fourier transform infrared spectroscopy (FTIR) using a Bruker Alpha II spectrometer (Bruker Optics GmbH & Co. KG, Ettlingen, Germany) in attenuated total reflectance (ATR) mode. Spectra were recorded in the wavenumber range of 4000–400 cm^{-1} at a resolution of 4 cm^{-1}. FTIR analysis was employed to identify changes in surface functional groups after thermal and alkaline modification, as well as after the sorption process.

Surface morphology and microstructure of the samples were examined by scanning electron microscopy (SEM) using a SEM5000Pro microscope (CIQTEK Co., Ltd., Hefei, Anhui, China). Elemental composition was determined by EDX analysis using an Oxford X-Max 80 (Oxford Instruments, Abingdon, UK) detector attached to the SEM system.

2.3. Determination of Specific Surface Area and Sorption Experiments

Specific surface area and pore characteristics of the samples were determined by low-temperature nitrogen adsorption–desorption measurements using a Sorbometr-M sorptometer (KATAKON, Novosibirsk, Russia). Prior to analysis, the samples were dried at 100 °C to constant weight and degassed in the instrument's sample preparation station. Adsorption–desorption isotherms were recorded at liquid nitrogen temperature (−196 °C), and the specific surface area was calculated using the Brunauer–Emmett–Teller (BET) method with the instrument software.

Sorption experiments were conducted using sorbent fractions of 0.5–2 mm. An aqueous NH_4Cl (Sigma-Aldrich, St. Louis, MO, USA) solution containing ammonium nitrogen (NH_4^+-N) was used as the model solution.

In all experiments, the solution volume was 100 mL.

Kinetic studies were carried out at an initial NH_4^+-N concentration of 20.99 mg/L over a contact time range of 30–240 min. An initial NH_4^+-N concentration of 20.99 mg/L was selected as a representative intermediate concentration within the studied range to obtain well-resolved kinetic curves and to compare the sorbents under identical non-saturating conditions.

The effect of pH was investigated within the range of 3–10. The influence of sorbent dosage was evaluated by varying the sorbent mass from 0.5 to 3.0 g.

Sorption isotherms were constructed at initial NH_4^+-N concentrations ranging from 10 to 50 mg/L.

The sorption process was performed in conical flasks under agitation on an orbital shaker at 200–250 rpm at room temperature (22–25 °C). The agitation speed was kept constant to ensure suspension homogeneity and to avoid additional variation from external mass-transfer effects.

After the contact time, the suspension was filtered, and the residual NH_4^+-N concentration in the filtrate was determined spectrophotometrically using a DR 3900 spectrophotometer (Hach, Loveland, CO, USA) with Nessler reagent (Hach, Loveland, CO, USA).

Particle size and ζ-potential of the samples were determined by dynamic light scattering (DLS) and electrophoretic light scattering using a Zetasizer Nano ZS analyzer (Malvern Panalytical, Malvern, UK).

The experimental data are reported as the mean ± standard deviation (SD) of three independent runs. Error bars are included in the graphical representations to indicate the measurement precision. The experimental error did not exceed 5%.

2.4. Adsorption Calculations and Mathematical Modeling

The quantitative parameters of the adsorption process, specifically the amount of ammonium adsorbed at time t (q_t, mg/g) (1) and at equilibrium (q_e, mg/g) (2), as well as the removal efficiency (R, %) (3), were calculated using the following mass balance equations [27]:

$$q_t = \frac{(C_0 - C_t)}{m} \times V \quad (1)$$

$$q_e = \frac{(C_0 - C_e)}{m} \times V \quad (2)$$

$$R_{(\%)} = \frac{(C_0 - C_e)}{C_o} \times 100 \quad (3)$$

where C_0, C_t, and C_e (mg/L) represent the initial, time-dependent (at time t), and equilibrium concentrations of ammonium, respectively; V (L) is the volume of the solution, and m (g) is the dry mass of the sorbent. All experimental data are reported as the mean of three independent replicates (n = 3) with standard deviation (SD).

To investigate the adsorption kinetics, the data were analyzed using the linearized forms of the pseudo-first-order (PFO) (4) and pseudo-second-order (PSO) (5) models. The equations are expressed as follows [28]:

$$In\ (q_e - q_t) = In(q_e) - k_1 t \quad (4)$$

$$\frac{t}{q_t} = \frac{1}{k_2 q_e^2} + \frac{t}{q_e} \quad (5)$$

where k_1 (1/min) and k_2 (g/mg·min) are the rate constants of the PFO and PSO models, respectively. The experimentally determined equilibrium capacity ($q_{e,exp}$) was used for linearization of the PFO model. For the PSO model, the calculated equilibrium capacity ($q_{e,calc}$) and the initial adsorption rate h (mg/g·min) (6) were determined from the slope and intercept of the t/q_t vs. t plot [27]:

$$h = K_2 q_e^2 \quad (6)$$

The equilibrium isotherms were fitted using the non-linear forms of the Langmuir (7) and the Freundlich (8) models [29]:

$$q_e = \frac{q_{max} k_L C_e}{1 + k_L C_e} \quad (7)$$

$$q_e = k_F C_e^{1/n} \quad (8)$$

where q_{max} (mg/g) is the maximum monolayer capacity; K_L (L/mg) is the Langmuir constant; K_F ((mg/g)(L/mg)$^{1/n}$) and n are Freundlich constants.

Mathematical modeling was performed using OriginPro 2024 (OriginLab Corporation, Northampton, MA, USA). Linear regression (least squares method) was used for kinetic models. Preliminary nonlinear regression was also tested; however, for the present dataset, the fitted parameters were unstable and sensitive to the initial estimates, which made the nonlinear solution less reproducible. Therefore, the linearized approach was retained as a transparent screening tool for model comparison under the available experimental conditions.

Non-linear curve fitting via the Levenberg–Marquardt algorithm was applied for isotherm models. The goodness-of-fit was evaluated primarily using the coefficient of determination (R^2).

Residual distributions were visually inspected to confirm the adequacy of model fitting.

2.5. Determination of the Point of Zero Charge (pHpzc)

The point of zero charge (pHpzc) for studying sorbents obtained by the pH drift method [30]. A series of 0.01 M NaCl (Sigma-Aldrich, St. Louis, MO, USA) solutions (100 mL each) was adjusted to initial pH values ranging from 2 to 11 in 1 unit increments by dropwise addition of 0.1 M HCl or 0.1 M NaOH. Prior to sorbent addition, the initial pH of each solution was recorded using a calibrated with a pH-150MI pH meter (Izmeritelnaya Tekhnika, Moscow, Russia). A sorbent mass of 0.5 g was added to each flask containing 100 mL of solution, after which the suspensions were agitated on an orbital shaker at 200 rpm for 24 h at room temperature (22 ± 1 °C); the flasks were kept tightly sealed throughout. The exact pHpzc value was calculated by linear interpolation between two adjacent points at which ΔpH changes sign. All measurements were performed in triplicate.

3. Results and Discussion

3.1. Mineral Composition of the Starting Materials

The results of the XRF analysis showed that the diatomite from the Aktobe region is characterized by a high content of silicon dioxide (SiO_2), the content of which is 82.60% (Table 1). The second most important components are Al_2O_3 (8.65%) and Fe_2O_3 (2.80%), which are present in the form of aluminosilicate and iron-containing phases. The concentration of TiO_2 (1.33%) and MgO (~1.10%) indicates the presence of mineral impurities typical of diatomites of natural origin (Table 1).

Table 1. The content of chemical compounds in natural diatomite and zeolite.

Component	Concentration, *w*/*w* %, (±0.01)	
	Diatomite	Zeolite
SiO_2	82.60	67.01
Al_2O_3	8.65	14.50
Fe_2O_3	2.80	4.51
MgO	1.10	2.12
K_2O	0.60	4.03
CaO	0.10	6.40
TiO_2	1.33	0.30
Na_2O	1.30	4.70
P_2O_5	0.03	0.17
SO_3	0.20	-
V_2O_5	0.03	-
Cl	0.92	-
Cr_2O_3	0.02	-
MnO	-	0.06

The natural zeolite of the Shankhanai deposit is characterized by a more variable and chemically complex oxide composition compared to diatomite [31–34]. The main structure-forming component is silica (SiO_2), the content of which is 67.01%, reflecting the high degree of silicatization of the crystalline framework and the inherent aluminosilicate nature of zeolites. The second oxide in terms of content is Al_2O_3 (14.50%), which provides the basis of the tectosilicate structure and determines the cation-exchange properties of the mineral.

The Fe_2O_3 content in zeolite is significantly higher than in diatomite and can range 4.51%, which indicates the presence of iron-containing phases. The concentrations of MgO (2.12%) and K_2O (4.03%) indicate the variability of impurity minerals and sorbed cations due to the geochemical features of the deposit. The presence of alkaline earth oxide—CaO

(6.40%)—reflects the ability of zeolites to include cations of various valences in the structure due to a highly developed ion exchange system.

The content of TiO_2 (0.30%), Na_2O (4.70%) and P_2O_5 (0.17%) indicates the presence of accessory mineral phases and possible adsorbed compounds of a phosphate nature. The concentrations of MnO (0.06%) also confirm the presence of manganese impurities typical of aluminosilicate rocks of volcanogenic or hydrothermal origin.

3.2. Optimization of Obtaining Sorbents from Diatomite

The chemical composition of diatomite remained stable over the temperature range up to 750 °C (Table 2). The SiO_2 content varied within 83.41–83.70 wt.%, confirming the siliceous nature of the material. Changes in the concentrations of minor oxides (Al_2O_3, Fe_2O_3, MgO, Na_2O, and K_2O) were insignificant and are likely associated with dehydration and redistribution of surface components rather than alterations in the bulk composition.

Table 2. The content of chemical compounds in natural diatomite at different degrees of calcination.

Component	Concentration, *w*/*w* %, (±0.01)				
	Temperature, °C				
	200	**450**	**550**	**650**	**750**
SiO_2	83.41	83.70	83.60	83.52	83.47
Al_2O_3	8.63	8.30	8.5	8.6	8.5
Fe_2O_3	2.63	2.63	2.70	2.64	2.50
MgO	1.09	1.10	1.11	1.12	1.11
K_2O	0.81	0.60	0.50	0.66	0.54
CaO	0.21	0.20	0.22	0.30	0.30
TiO_2	1.21	1.32	1.30	1.20	1.20
Na_2O	1.05	1.22	1.38	1.36	1.30
P_2O_5	0.03	0.03	0.02	0.02	0.01
SO_3	0.3	0.3	0.3	0.4	0.4
V_2O_5	0.02	-	0.02	0.03	0.02
Cl	0.5	0.2	0.03	0.01	0.01
Cr_2O_3	-	0.02	-	0.01	-

Thus, heat treatment up to 750 °C does not significantly alter the chemical composition of diatomite within the accuracy limits of the XRF method.

XRD phase analysis showed that quartz and alumosilicate minerals of a clay nature predominate in all samples (Figure 1a). There were no significant changes in the phase composition in the range up to 750 °C. The observed changes in the relative peak intensities may be related to the dehydration of clay minerals and a change in their degree of order, but the appearance of new crystalline phases or complete amorphization has not been recorded.

The FTIR spectra of the pristine and thermally treated diatomite samples display a set of bands characteristic of siliceous materials, corresponding to vibrations of the silicon-oxygen framework (Figure 1b). In all cases, the most intense band appears in the 1006–1027 cm^{-1} range (absorbance ≈ 0.15), which corresponds to the asymmetric stretching vibrations of Si-O-Si linkages and indicates preservation of the structural backbone of amorphous silica regardless of the treatment temperature [35,36].

Bands at 423–452 cm^{-1} (absorbance ≈ 0.06) are observed in the low-frequency region and are attributable to O-Si-O deformation (bending) vibrations, a feature also typical of a siliceous framework. The intensity and position of these bands remain essentially unchanged, indicating high thermal stability of the SiO_4 structural units [36].

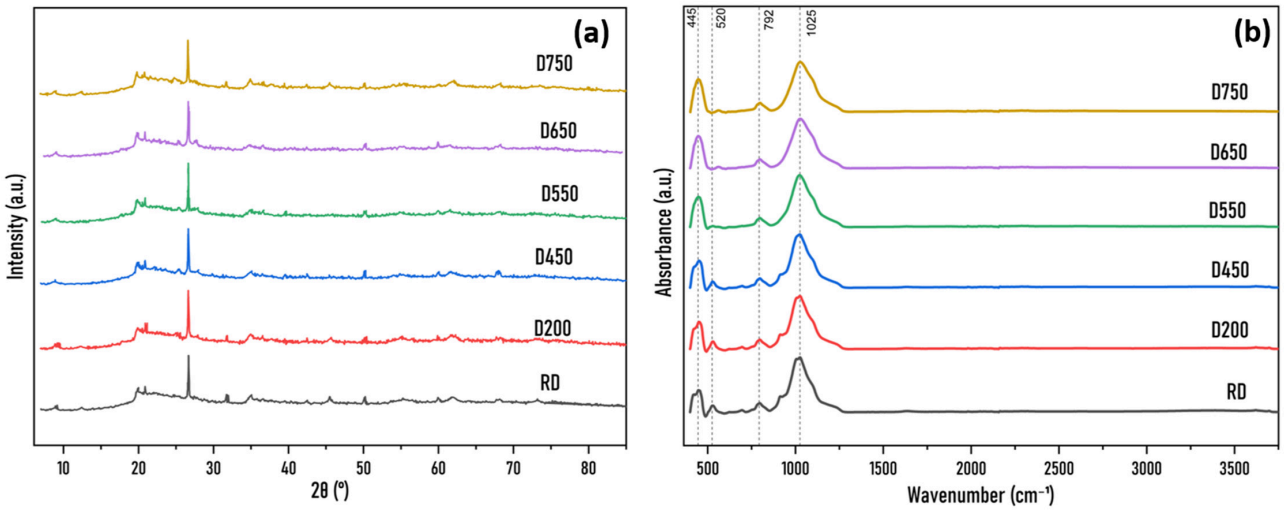


Figure 1. (**a**) XRD images and (**b**) IR spectra of natural and thermally treated diatomite at different calcination temperatures (200, 450, 550, 650, and 750 °C). Note: the identified phases and the corresponding PDF reference cards are provided in Tables S1 and S2 in the Supplementary Material.

Additional weak bands are observed at 528–560, 621–622, 695–696, and 797–798 cm^{-1}. These features are characteristic of various symmetric and deformation vibrations associated with siliceous and clay phases present in the natural diatomite. Their low intensity and reproducibility between samples confirm the absence of significant structural transformations upon heating.

Comparison of spectra for samples calcined over the 200–750 °C range with the untreated material shows that thermal treatment within this range does not produce a noticeable shift in the principal Si-O-Si and O-Si-O bands. Minor band shifts (<3 cm^{-1}) were detected; these are within the instrumental resolution and do not indicate substantial structural reorganization.

Analysis of the specific surface area and porosity of the diatomite revealed a pronounced dependence of textural parameters on the thermal treatment temperature (Table 3). The as-received sample exhibited a specific surface area of 34.25 m^2/g and a total pore volume of 0.034 cm^3/g. Heating to 200 °C produced a slight increase in surface area (to 35.60 m^2/g), which can be attributed to the removal of physically adsorbed moisture and opening of previously inaccessible pores.

Table 3. Specific surface area and pore volume of diatomite at different calcination temperatures.

Samples	Natural Diatomite	200 °C	450 °C	550 °C	650 °C	750 °C
Specific surface area, (m^2/g)	34.25	35.60	46.32	41.27	26.73	16.77
Pore volume, (cm^3/g)	0.034	0.057	0.179	0.129	0.045	0.039
V_{mic}, (cm^3/g)	0.001	0.005	0.012	0.010	0.008	0.006
V_{meso}, (cm^3/g)	0.033	0.052	0.167	0.110	0.037	0.033

The most pronounced changes were recorded in the 450–550 °C interval. At 450 °C the specific surface area increased to 46.32 m^2/g and the total pore volume reached a maximum of 0.179 cm^3/g. Similar values persisted at 550 °C (41.27 m^2/g and 0.129 cm^3/g, respectively). The increase in textural parameters in this temperature interval may be due to the removal of structurally bound water, partial dehydroxylation of clay components, disruption of interparticle contacts, and the development of additional mesoporosity.

Importantly, these changes occur without significant restructuring of the crystalline framework, as confirmed by XRD and FTIR results; therefore, the thermal treatment predominantly affects texture rather than phase composition.

At higher temperatures (650 °C and above) the specific surface area decreased to 26.73 m^2/g with a pore volume of 0.045 cm^3/g; at 750 °C the reduction became more pronounced (16.77 m^2/g and 0.039 cm^3/g, respectively). These observations are consistent with the findings reported in [37]. The decline in textural characteristics at elevated temperatures may be associated with partial sintering of particles, densification of the structure, condensation of siloxane (Si-O-Si) bonds, and a reduction in accessible pore volume.

Analysis of the textural data for diatomite samples (Table 3) reveals a significant non-linear relationship between the calcination temperature and the development of the pore structure. The total pore volume increased more than fivefold, from 0.033 cm^3/g in the raw sample to a maximum of 0.179 cm^3/g at 450 °C. This growth is predominantly attributed to the expansion of the mesopore network reaching 0.167 cm^3/g, accounting for over 93% of the total porosity. The sharp increase in V_{meso} at 450 °C is explained by the removal of structurally bound water, which effectively clears the entrance to the internal channels and siloxane (Si-O-Si) framework. Thermal activation at 450 °C also resulted in a 12-fold increase in the micropore volume from 0.001 to 0.012 cm^3/g, which is attributed to the removal of impurities and moisture from the mineral's internal structure. Nevertheless, the contribution of micropores to the total porosity remains insignificant (less than 7%), confirming the predominantly mesoporous nature of the modified diatomite. These observations are consistent with the findings reported in [37]. However, increasing the temperature to 750 °C leads to a drastic reduction in V_{meso} to 0.027 cm^3/g due to the sintering of the silica skeleton and the collapse of the thin-walled pores.

The increase in adsorption performance at 450–550 °C is best interpreted as a textural opening of the diatomite structure rather than a bulk structural transformation, since the XRD and FTIR data indicate preservation of the siliceous framework. At higher temperatures partial degradation of textural properties occurs due to thermal densification of the material.

Based on the data obtained, the sample calcined at 450 °C was selected for subsequent alkaline activation and sorption experiments, since within the investigated temperature range it provided the best balance between textural development and preservation of the siliceous framework. In particular, this sample showed the highest specific surface area (46.32 m^2/g) and the largest pore volume (0.179 cm^3/g), while XRD indicated preservation of the mineral structure and FTIR showed no significant changes in the silica matrix.

3.3. Structural and Morphological Characteristics of Natural and Modified Sorbents

In order to assess the effect of the modification on the structural and morphological characteristics, phase composition and specific surface area of sorbents, as well as for comparison with the initial samples, FTIR, XRD and specific surface area measurement were performed.

3.3.1. Surface Morphology (SEM Analysis)

SEM images of natural samples emphasize their structural differences (Figure 2). Natural diatomite is characterized by distinct frustules with a perforated framework of biogenic silica, which contributes to its porous morphology. Natural zeolite, on the contrary, consists of dense irregular crystalline aggregates typical of aluminosilicate minerals with a more compact and rigid microstructure.

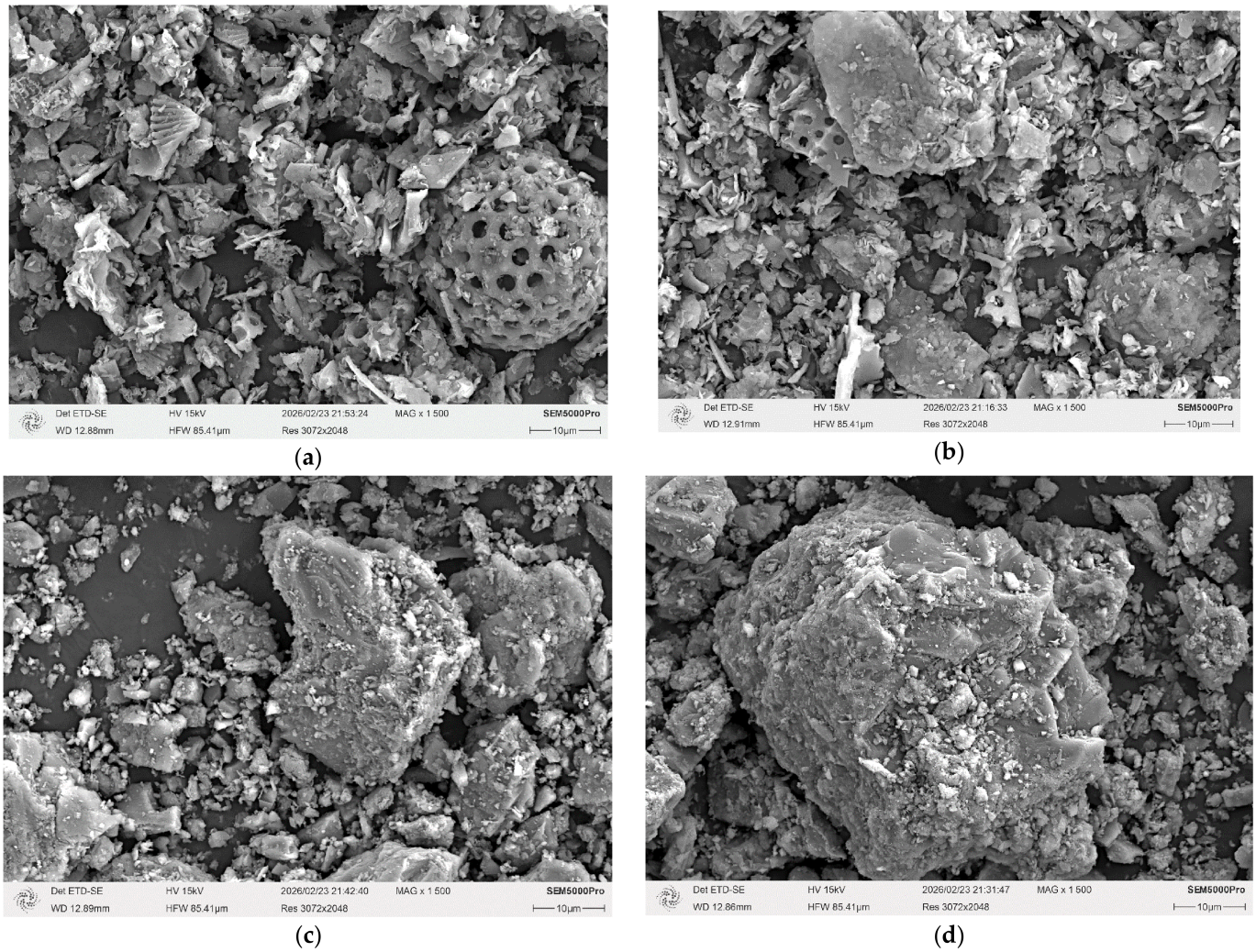


Figure 2. SEM micrographs of the studied sorbents (magnification ×1500): (**a**) natural diatomite, (**b**) diatomite modified with NaOH, (**c**) natural zeolite and (**d**) zeolite modified with NaOH.

SEM micrographs show that treatment with 0.5 M NaOH solution does not cause significant morphological destruction of any of the minerals.

Well-preserved frustrated structures with characteristic perforations are observed in natural diatomite. After the alkaline treatment, the general geometry of the frustrations remains unchanged; however, a slight surface roughness and a less defined outline of the edges can be noticed, which may indicate a change in the surface.

Natural zeolite has dense crystalline aggregates similar to the blocks typical of aluminosilicate frameworks. After treatment with NaOH, there is no significant morphological destruction, which allows for the preservation of the crystal structure on a micro scale. Minor changes in the surface texture may reflect surface-level modification rather than structural destruction.

Overall, the SEM results indicate that treatment with 0.5 M NaOH modifies the surface features of both materials without causing macroscopic structural collapse. From a practical perspective, this is important because it suggests that the improved adsorption performance observed after alkaline modification is mainly associated with surface-level chemical changes, such as the formation and redistribution of reactive hydroxyl groups, rather than with major reconstruction of the mineral framework. In the case of diatomite, the slight surface roughening observed after NaOH treatment is consistent with partial etching of the silica surface, which can increase the density of Si–OH groups and thereby promote

interaction with NH_4^+ [22–24]. For zeolite, the preservation of the crystalline aggregate morphology under alkaline conditions is consistent with the stability of the aluminosilicate framework at 0.5 M NaOH, as also supported by the XRD results in Section 3.3.2. This suggests that the modest improvement in adsorption performance after modification is likely related to surface-level cation redistribution rather than to structural reorganization of the framework.

3.3.2. Analysis of Functional Groups and Phase Composition (FTIR and XRD)

The FTIR spectra of diatomite are dominated by an intense band at approximately ~1025 cm^{-1}, characteristic of asymmetric stretching vibrations of Si-O-Si bonds in silica (Figure 3a). After treatment with 0.5 M NaOH, a noticeable low-wavenumber shift in this band to ≈997 cm^{-1} is observed, accompanied by changes in its shape and relative intensity. In addition, absorption in the lower-frequency region (~450 cm^{-1}) becomes more pronounced in the modified sample, and variations are evident around ~798 cm^{-1}. These differences indicate restructuring of the local chemical environment of siloxane bonds and the formation or redistribution of surface functional groups, consistent with the known effect of alkaline treatment on the Si-O-Si stretching vibration and the multiplication of surface Si-OH groups in amorphous silica [35,38].

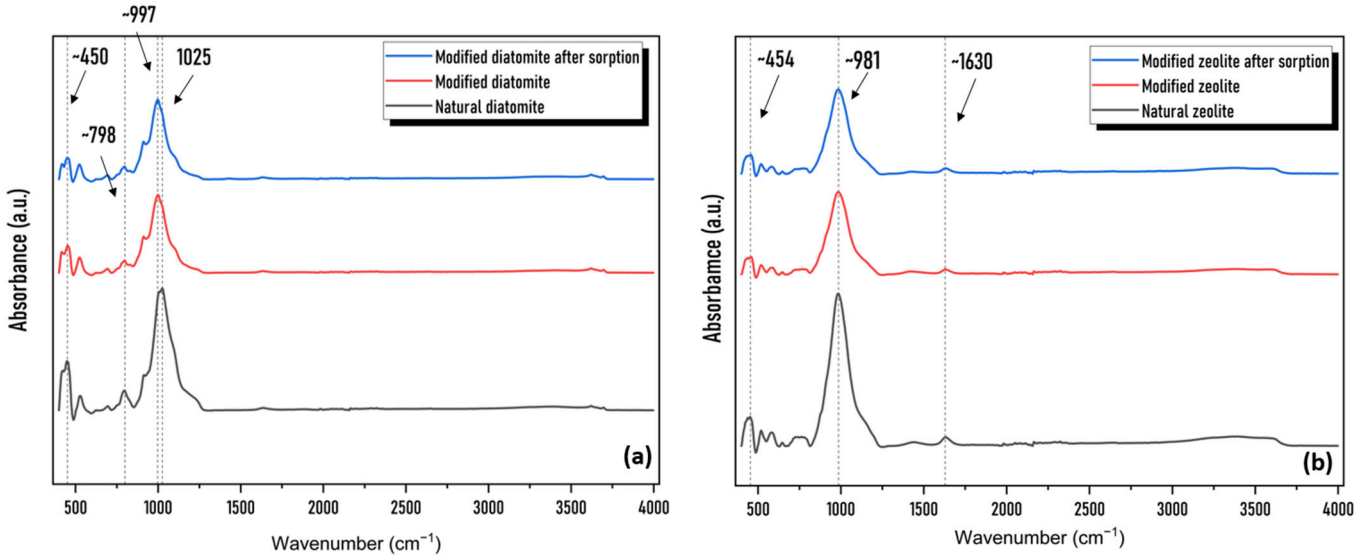


Figure 3. FTIR spectra of the investigated sorbents before, after modification and after sorption experiments with 0.5 M NaOH: (**a**) diatomite and (**b**) zeolite.

In the FTIR spectra of zeolite (Figure 3b), the main framework band appears at approximately ~981 cm^{-1}. After alkaline treatment, the shift in this band is minimal (~2 cm^{-1}), and the overall spectral shape and relative intensities remain comparable to those of the untreated material. A distinct band near ~1630 cm^{-1} corresponds to adsorbed water within the zeolite pores [39]. Thus, FTIR analysis suggests that alkaline modification more significantly alters the surface chemical environment of amorphous diatomite, whereas the zeolite framework structure remains relatively stable.

The XRD patterns of the pristine and alkali-modified diatomite (Figure 4a) show the dominance of amorphous silica, evidenced by a broad diffuse halo in the low 2θ region with several weak, sharp reflections corresponding to minor crystalline impurities. After thermal and 0.5 M NaOH treatment, the positions of the main features and the overall diffraction profile remain essentially unchanged. No new crystalline phases are formed, and variations in the intensities of minor reflections are likely associated with the removal

of surface impurities or redistribution of small amounts of crystalline components. Taken together with the textural and FTIR results, these findings indicate that the modification primarily affects the surface chemistry and pore structure, while the bulk SiO_2 matrix remains structurally stable.

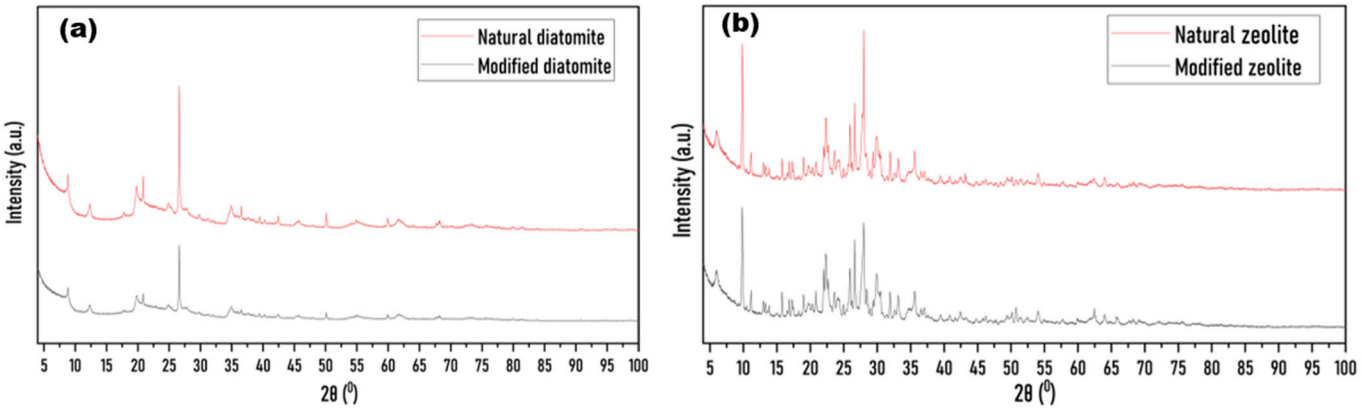


Figure 4. X-ray diffraction (XRD) patterns of: (**a**) raw and modified diatomite; (**b**) raw and modified zeolite.

Diffractograms of natural and modified zeolites are characterized by a set of clear sharp reflexes typical of a crystalline aluminosilicate lattice (Figure 4b). After 0.5 M NaOH treatment, the positions and relative intensities of the main reflexes remain unchanged, which indicates the preservation of the crystal structure under the selected modification conditions. The observed slight variations in the intensities of individual peaks may reflect surface changes or local redistribution of cations within the pore network, but there are no obvious signs of the formation of new phases or the destruction of the framework.

3.3.3. Elemental Surface Composition (EDX Analysis)

Representative EDX spectra of the sorbent surfaces before and after alkaline modification are shown in Figure 5. Natural diatomite was dominated by Si and O, with minor amounts of Al, Fe, Mg, Na, K, Ca, and Ti, which is consistent with the siliceous matrix containing small aluminosilicate impurities. After treatment with 0.5 M NaOH, the elemental composition of diatomite remained Si-rich, while the Na signal was not detected on the analyzed surface (Table 4). This suggests that alkaline treatment did not result in sodium retention, but rather promoted surface leaching and rearrangement of the outer silica layer. The slight increase in Al and Fe on the modified surface is consistent with local heterogeneity of the natural material and with partial exposure of impurity-rich domains after alkaline etching.

Table 4. EDX composition of diatomite: natural vs. NaOH-modified.

Element	Natural Diatomite (Wt.%)	Natural Diatomite (At.%)	Modified Diatomite (Wt.%)	Modified Diatomite (At.%)
O	54.91	68.47	50.83	65.58
Na	0.78	0.68	-	-
Mg	0.82	0.67	1.29	1.09
Al	4.84	3.58	6.23	4.76
Si	35.77	25.41	35.42	26.03
K	0.78	0.40	0.81	0.43
Ca	0.21	0.11	0.56	0.29
Ti	0.18	0.07	0.38	0.16
Fe	1.72	0.61	4.48	1.66
Total	100.00	100.00	100.00	100.00

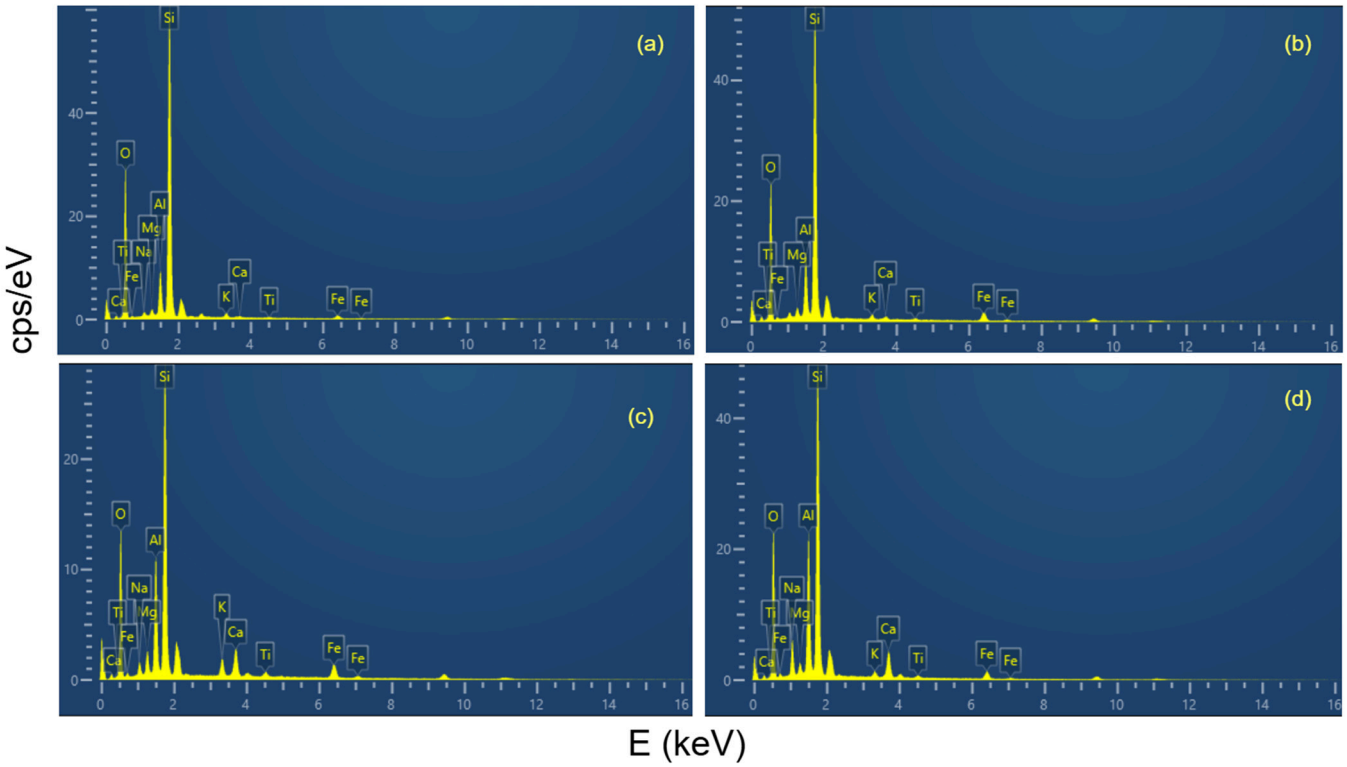


Figure 5. EDX spectra of: (**a**) natural diatomite, (**b**) diatomite modified with 0.5 M NaOH, (**c**) natural zeolite, and (**d**) zeolite modified with 0.5 M NaOH.

Natural zeolite showed a typical aluminosilicate composition, with appreciable Si, O, Al, and exchangeable cations, particularly Ca and Na. After alkaline modification, the Na content increased markedly (Table 5), whereas the Ca content decreased, indicating partial cation exchange at the zeolite surface. No new elements appeared after treatment, and the aluminosilicate framework remained intact, in agreement with the XRD results.

Table 5. EDX composition of zeolite: natural vs. NaOH-modified.

Element	Natural Zeolite (Wt.%)	Natural Zeolite (At.%)	Modified Zeolite (Wt.%)	Modified Zeolite (At.%)
O	46.61	62.13	45.70	60.16
Na	1.81	1.68	4.84	4.43
Mg	2.26	1.98	1.12	0.97
Al	9.75	7.70	11.66	9.10
Si	27.56	20.93	28.97	21.72
K	2.17	1.18	0.73	0.40
Ca	3.89	2.07	3.75	1.97
Ti	0.86	0.38	0.45	0.20
Fe	5.09	1.94	2.79	1.05
Total	100.00	100.00	100.00	100.00

Overall, the EDX data support two distinct responses to alkaline treatment: surface rearrangement of the siliceous diatomite matrix and cation exchange in zeolite.

3.3.4. Textural Characteristics and Specific Surface Area

Table 6 shows that heat-treated diatomite already has a significantly higher specific surface area than zeolite (46.32 natural diatomite (after calcination), 21.80 m^2/g for natural zeolite). After NaOH treatment, different effects are observed for the two materials: for

zeolite, the specific surface area increased from 21.80 to 25.65 m^2/g, and the pore volume increased from 0.0116 to 0.0157 cm^3/g, indicating a slight opening of the pore structure and the formation of additional available porosity. In diatomite, the change in texture parameters after the same treatment turned out to be insignificant: increased from 46.32 to 47.23 m^2/g, and the total pore volume decreased slightly from 0.179 to 0.175 cm^3/g.

Table 6. Specific surface area and pore volume of raw and NaOH-modified diatomite and zeolite.

Samples	Natural Zeolite	Modified Zeolite	Natural Diatomite (After Calcination)	Modified Diatomite
Specific surface area (m^2/g)	21.80	25.65	46.32	47.23
Pore volume (cm^3/g)	0.012	0.016	0.179	0.175
V_{mic}, (cm^3/g)	0.001	0.005	0.012	0.011
V_{meso}, (cm^3/g)	0.011	0.011	0.167	0.164

The nitrogen adsorption–desorption isotherms for the four adsorption-relevant samples are provided in the Supplementary Material (Figure S1).

According to the textural data in Table 6, modified diatomite exhibits a predominantly mesoporous structure with a V_{meso} of 0.164 cm^3/g, representing over 94% of its total porosity. In contrast, modified zeolite remains significantly microporous (~33% of total pore volume), which creates higher diffusion resistance for ammonium ions compared to the open pore network of diatomite.

This pattern is consistent with the fact that alkaline activation of 0.5 M NaOH modifies the pore system of zeolites to a greater extent (partial opening), whereas for highly developed amorphous diatomite, the main effect is probably a change in surface properties (purification, formation/redistribution of functional groups), rather than a radical change in texture. Consequently, the increase in the sorption activity of modified zeolite can be partially explained by an increase in the available surface and pore volume, whereas the superiority of modified diatomite in a number of sorption parameters is more likely due to a combination of its already high initial area and changes in surface chemistry, rather than a large increase in the specific surface parameters.

3.4. Sorption Properties of NH_4^+-N

3.4.1. Effect of Contact Time and Kinetic Modeling

The sorption of NH_4^+-N on all investigated samples exhibited a rapid initial stage followed by a slower approach to equilibrium (Figure 6a). During the first 60 min, a sharp increase in sorption capacity (q_t) was observed, indicating rapid occupation of readily accessible active sites on the surface of the materials. Subsequently, the sorption rate decreased noticeably, and dynamic equilibrium was reached by approximately 120 min, as evidenced by the plateau in q_t values. Further extension of the contact time did not result in a statistically significant increase in sorption capacity. The modified forms of diatomite and zeolite consistently demonstrated higher q_t values throughout the entire experimental period compared with their respective natural counterparts.

Accordingly, the kinetic parameters should be interpreted as comparative descriptors of model performance rather than as absolute optimized constants.

The kinetic curves show a fast initial uptake followed by a gradual approach to equilibrium, which is typical of adsorption processes where abundant external sites are occupied first and the rate then decreases as these sites become saturated. The somewhat higher initial rate observed for modified diatomite is consistent with the textural improvement caused by thermal and alkaline treatment, including the development of a more accessible pore structure. For the later stage of the process, the rate decrease likely reflects the

progressive filling of available sites and increasing diffusion resistance within the particle interior. In this sense, the kinetic differences between the materials are better interpreted as a consequence of surface accessibility and pore structure than as evidence of a single controlling mechanism.

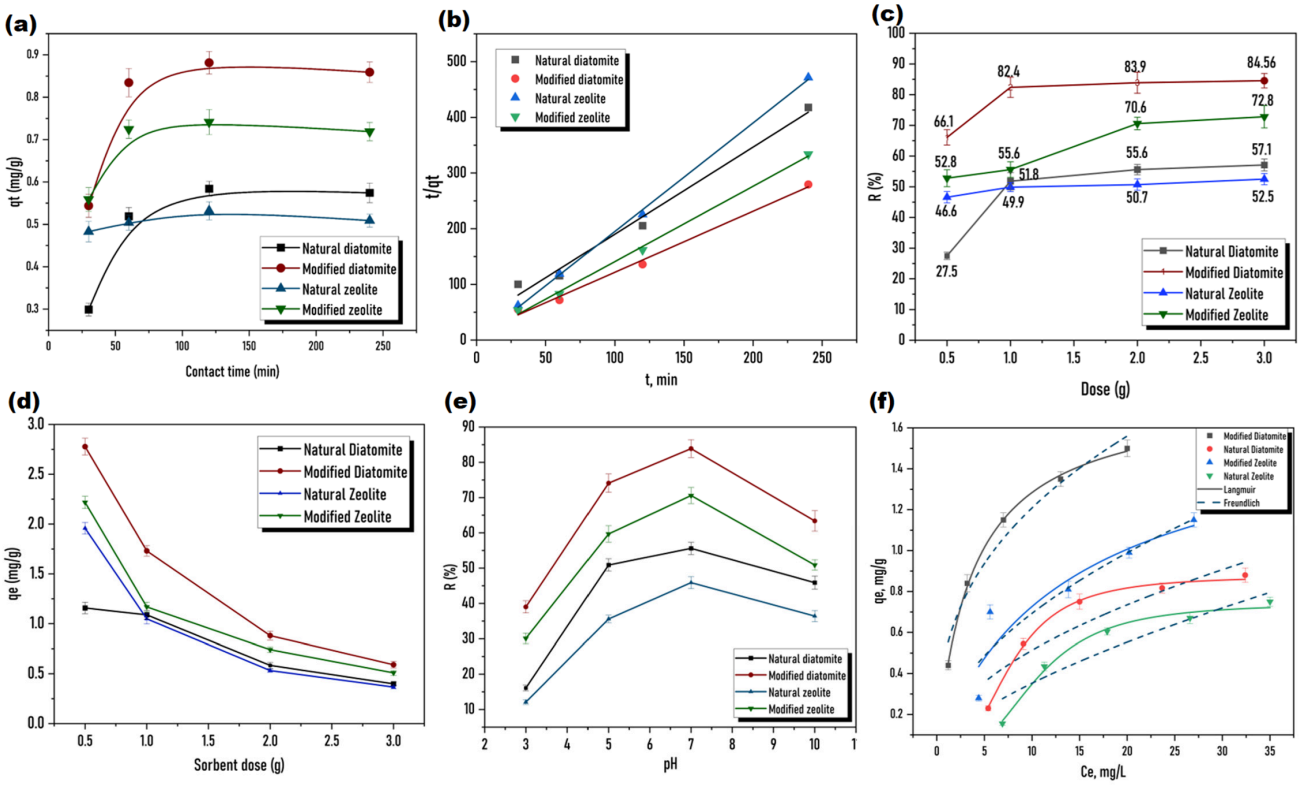


Figure 6. NH_4^+-N adsorption performance of natural and modified diatomite and zeolite under controlled batch conditions: (**a**) effect of contact time (30–240 min) at a fixed sorbent dose (2 g), initial pH (7), and initial NH_4^+-N concentration (20.99 mg/L); (**b**) pseudo-second-order kinetic model fits; (**c**) effect of sorbent dosage (0.5–3 g) on NH_4^+-N removal efficiency at a fixed contact time (120 min), initial pH (7), and initial concentration (20.99 mg/L); (**d**) effect of sorbent dosage on equilibrium adsorption capacity under the same conditions; (**e**) effect of initial solution pH (3–10) at a fixed sorbent dose (2 g), contact time (120 min), and initial concentration (20.99 mg/L); and (**f**) Langmuir and Freundlich isotherm fits at a fixed sorbent dose (2 g), contact time (120 min), and initial pH (7).

The kinetics of the process were analyzed using the PFO and PSO models. Comparative evaluation demonstrated that the PSO model provided a superior fit to the experimental data: the coefficient of determination (R^2) for PSO ranged from 0.997 to 0.999, whereas for the PFO model it varied between 0.72 and 0.94 (Table 7). While the PSO model fits the data with high precision ($R^2 > 0.99$), it should be noted that such mathematical agreement is an indicator of surface-controlled processes rather than definitive proof of a specific chemical mechanism [40,41].

Table 7. Kinetic parameters of pseudo-first-order and pseudo-second-order models for ammonium adsorption onto natural and modified diatomite and zeolite.

Sorbent	$q_{e,exp}$ (mg/g)	R^2 (PFO)	$q_{e,calc}$ (mg/g)	k_2 (g/mg·min)	h (mg/g·min)	Δq_e (%)	R^2 (PSO)
Natural Diatomite	0.584	0.94	0.60	0.042	0.0151	2.7%	0.998
Modified Diatomite	0.881	0.91	0.89	0.021	0.0166	1.0%	0.999
Natural Zeolite	0.532	0.72	0.54	0.031	0.0090	1.5%	0.997
Modified Zeolite	0.741	0.88	0.75	0.025	0.0141	1.1%	0.999

Additional confirmation of the adequacy of the PSO model is provided by the close agreement between the calculated and experimental equilibrium adsorption capacities. The relative deviation between $q_{e,calc}$ and $q_{e,exp}$ (%Δq_e) did not exceed 1.0–2.7%, indicating excellent agreement between the model and the experimental data.

Among the studied samples, modified diatomite showed the highest h value (0.0166 mg·g^{-1}·min^{-1}), which indicates a higher rate of initial ion capture compared to other sorbents.

A more accurate description of the kinetic data by the PSO model suggests that the sorption process is consistent with surface-controlled interactions on the sorbent surface (Figure 6a). However, it should be noted that compliance with the PSO model is not in itself a direct proof of the mechanism of chemosorption.

3.4.2. Effect of Sorbent Dose

The removal efficiency of NH_4^+-N depended strongly on sorbent dosage (Figure 6c). Increasing the sorbent mass from 0.5 to 3.0 g resulted in a clear improvement in solution purification for all investigated samples. The steepest increase in removal efficiency was observed in the low-dose region (0.5–1.0 g), after which the growth became less pronounced and gradually approached a plateau at higher dosages. Under the studied conditions, modified diatomite showed the most favorable response to dosage increase, reaching 84.56% removal at 3.0 g, whereas natural zeolite exhibited the lowest sensitivity to increasing sorbent mass, reaching 52.5% at the same dose. The differences between natural and modified materials were statistically significant ($p < 0.05$), confirming the positive effect of alkaline activation on sorption performance.

At the same time, the equilibrium adsorption capacity (q_e, mg/g at 120 min) showed the opposite trend (Figure 6d): as the sorbent dose increased, q_e decreased for all materials. This behavior is typical for batch systems operated at a fixed initial solute concentration, where the same amount of ammonium is distributed over a progressively larger mass of sorbent. In other words, increasing the dose improves overall removal efficiency but lowers the amount adsorbed per gram of material.

This trade-off between removal efficiency and specific adsorption capacity indicates that dose selection should be treated as an operational optimization problem rather than a simple maximization of one parameter. Higher dosages favor greater purification of the solution, whereas lower dosages make more efficient use of the intrinsic sorption capacity of the material.

3.4.3. Effect of pH

Solution pH is a key parameter governing both the state of surface functional groups of the sorbents and the chemical speciation of ammonium nitrogen in aqueous media [41,42]. In the present study, the effect of acidity was evaluated within the pH range of 3–10 (Figure 6e).

A consistent trend was observed for all samples: the lowest removal efficiencies occurred under acidic conditions (pH 3), the efficiency increased significantly toward neutral values (maximum around pH 7), and decreased again under alkaline conditions (pH 10). For modified diatomite and modified zeolite, the maximum removal efficiencies at pH ≈ 7 reached 83.9% and 70.6%, respectively, whereas at pH 3 the efficiency decreased to 12–39%. Such behavior is consistent with previously reported trends for ammonium adsorption on aluminosilicate and carbon-based sorbents [21,43,44].

At low pH values, the high concentration of protons (H^+) leads to competition with NH_4^+ cations for active sites on the sorbent surface, thereby reducing adsorption efficiency [37]. Additionally, protonation of surface functional groups occurs, decreasing the

number of negatively charged sites available for electrostatic interaction. The ammonium system is characterized by an acid-base equilibrium with pKa ≈ 9.25. As pH approaches this value, a significant fraction of ammonium converts into uncharged molecular ammonia (NH_3) [21,43]. Since electrostatic adsorption and ion exchange require a charged adsorbate, this transformation results in a sharp decline in sorption efficiency.

A fundamental difference in binding mechanisms between the investigated materials should be emphasized. In zeolites, the negative framework charge originates from the structural features of the aluminosilicate lattice; therefore, ion exchange represents the dominant interaction pathway. In contrast, for diatomite, surface functional groups play a key role, and their charge state directly depends on the external pH.

Thus, near-neutral conditions provide the most favorable environment, ensuring a high fraction of ionic ammonium species and an optimal surface charge state of the sorbents.

3.4.4. Determination of the Point of Zero Charge (pHpzc)

To elucidate the adsorption mechanism and interpret the dependence of NH_4^+ removal efficiency on pH, the point of zero charge (pHpzc) was determined for all investigated sorbents. The pHpzc is defined as the pH value at which the net electrical charge of the surface is zero. Figure 7 presents the determination of the point of zero charge by the pH drift method over the pH range of 2 to 11.

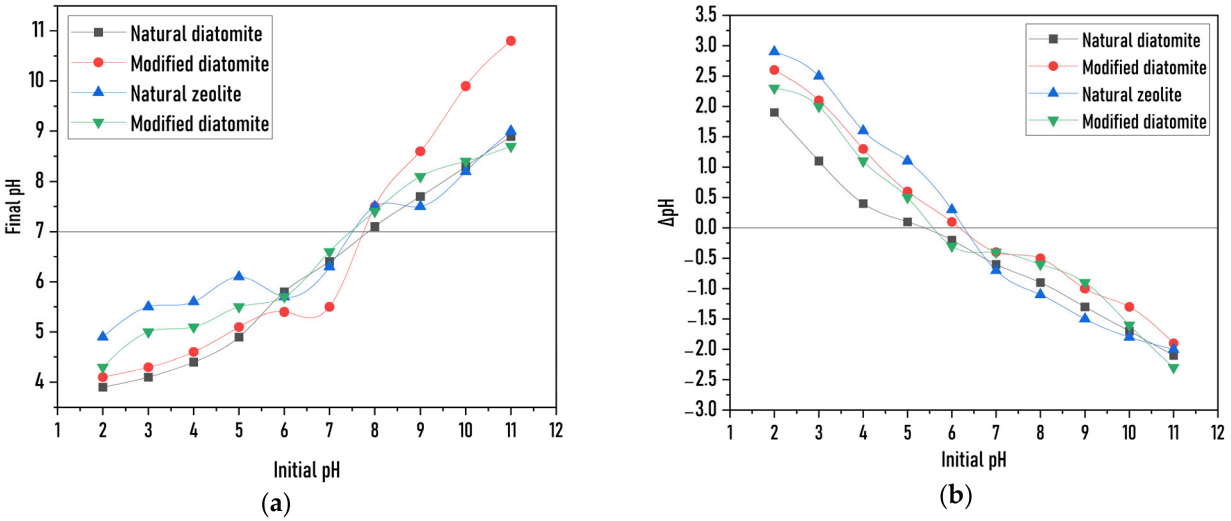


Figure 7. Determination of the point of zero charge by the pH drift method: (**a**) final pH as a function of initial pH for natural diatomite, modified diatomite, natural zeolite, and modified zeolite; (**b**) ΔpH as a function of initial pH for the same sorbents.

Based on the obtained data, the pHpzc values were determined as the intersection points of the ΔpH = f(pH_0) curves with the ΔpH = 0 line.

The pHpzc value of natural diatomite was 5.3, modified diatomite—6.3, natural zeolite—6.2, and modified zeolite—5.6. The obtained values are consistent with the data reported by [45,46], who established the pHpzc of natural zeolite in the range of 6.24–6.47. Minor differences in the absolute pHpzc values are attributed to differences in the mineralogical properties of materials from different deposits. Furthermore, ref. [21] demonstrated that the optimal pH range for ammonium adsorption on zeolite is 6 to 8, where the adsorption rate is maximum. Beyond this range, ammonium removal decreases markedly.

The higher pHpzc of the modified diatomite relative to the natural sample is attributed to the enrichment of the surface with Si–OH hydroxyl groups formed upon alkaline treat-

ment with 0.5 M NaOH [22,23]. An opposite trend was observed for zeolite: the pHpzc of the modified sample is slightly lower than that of the natural one, which may be associated with the redistribution of surface cations during alkaline treatment.

Correlation of the pHpzc values with the NH_4^+ removal efficiency profiles provides a consistent mechanistic explanation for the observed dependencies. At pH 3, well below the pHpzc of all sorbents (5.3–6.3), the surface carries a positive charge, resulting in electrostatic repulsion of NH_4^+ cations; additionally, the elevated H^+ concentration competes with NH_4^+ for active sites—the combination of these factors accounts for the minimum removal efficiency values observed (12–39%). At pH 7, exceeding the pHpzc of all investigated sorbents, the surface acquires a negative charge favorable for electrostatic attraction of NH_4^+ cations; under these conditions, ammonium exists predominantly in ionic form (pH << pKa = 9.25), which accounts for the maximum removal efficiency of 83.9% and 70.6% for modified diatomite and zeolite, respectively. The decline in efficiency at pH > 9 is attributable to the conversion of NH_4^+ to the uncharged form NH_3 (pKa ≈ 9.25), which reduces the proportion of charged adsorbate and weakens electrostatic interaction with the surface [41,42].

3.4.5. Adsorption Isotherms

To analyze the equilibrium behavior of the system and to evaluate the interaction mechanism between sorbate and the sorbent surface, the Langmuir and the Freundlich models were applied (Figure 6f). The Langmuir model assumes monolayer adsorption on an energetically homogeneous surface with a finite number of equivalent active sites, whereas the Freundlich model is empirical and accounts for surface heterogeneity and non-uniform distribution of adsorption energies.

Comparison of the determination coefficients (R^2) indicated that for modified diatomite, the Langmuir model provided the best fit to the experimental data (R^2 = 0.999). This suggests a more uniform distribution of active sites and the predominance of a monolayer adsorption mechanism within the studied concentration range. Similar observations—namely improved conformity to the Langmuir model after chemical or thermal modification of diatomite—have been reported in previous studies, where modified samples exhibited a more homogeneous adsorption surface and enhanced capacity.

For the natural minerals and modified zeolite, slightly higher R^2 values were obtained for the Freundlich model, indicating probable energetic heterogeneity of their surfaces. Nevertheless, the differences between the models are not substantial, and both approximations demonstrate satisfactory agreement with the experimental data (Table 8).

Table 8. Langmuir and the Freundlich isotherm parameters.

Sorbent	Model	q_{max} (mg/g)	K_L/K_F (mg/g)·(L/mg)$^{1/n}$	n	R_L	R^2
Mod. diatomite	Langmuir	1.758 ± 0.053 mg/g	0.275	-	0.068	0.999
Nat. diatomite	Freundlich	-	0.091	1.513	0.317	0.985
Mod. zeolite	Freundlich	-	0.163	1.649	0.267	0.755
Nat. zeolite	Freundlich	-	0.036	1.106	0.643	0.847

The dimensionless separation factor (R_L), calculated at the maximum initial concentration (C_0 = 50 mg/L), ranged from 0.068 to 0.643. Since for all systems the condition $0 < R_L < 1$ is satisfied, the adsorption process can be characterized as favorable within the investigated concentration range.

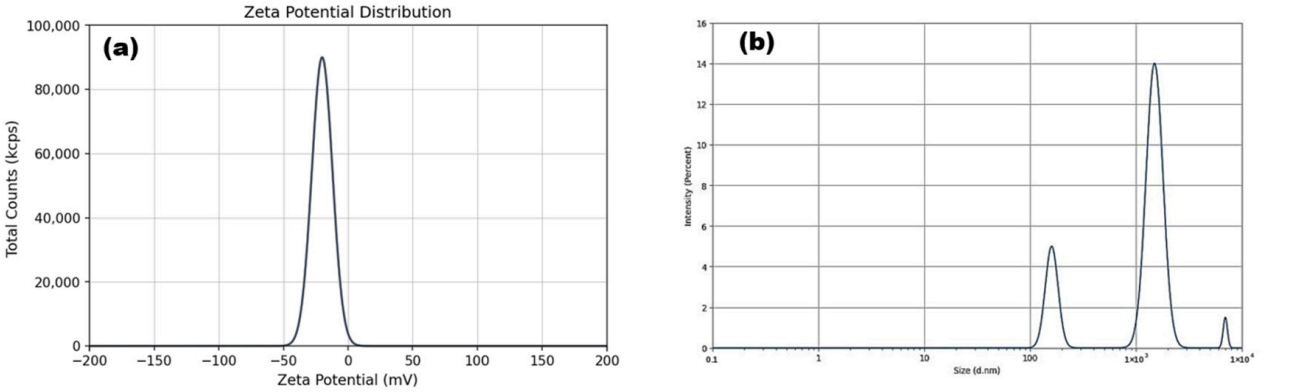
3.4.6. Comparative Performance

Comparative analysis of the sorption characteristics revealed that modified diatomite exhibited the best performance among the investigated materials. This sample achieved the highest ammonium removal efficiency (84.56%) and the largest calculated equilibrium capacity according to the Langmuir model (q_{max} = 1.758 mg·g^{-1}).

Although zeolites are traditionally regarded as efficient cation-exchange materials, under the conditions of the present experiment, their sorption performance was lower than that of the diatomite samples. This indicates that sorbent efficiency is determined not only by crystalline nature but also by structural features and the accessibility of active sites under specific aqueous conditions.

To obtain deeper insight into the behavior of diatomite in solution, additional characterization of its dispersed state was performed. According to DLS measurements, modified diatomite exhibited pronounced dispersion in water, forming particles with a hydrodynamic diameter of approximately 232 nm. This value is substantially smaller than the initial fraction size (0.5–2 mm), suggesting partial disaggregation or breakdown of aggregates upon contact with the solution. Increased dispersion likely enhances the effective surface area available for sorption. It should be emphasized that the 0.5–2 mm value refers to the dry sieve fraction used before sorption experiments, whereas DLS measures the hydrodynamic size of particles dispersed in water. Therefore, the smaller DLS size reflects partial disaggregation and formation of finer aggregates in the aqueous medium rather than a contradiction with the initial particle fraction.

The measured ζ-potential of the modified diatomite (−29.75 mV) indicates a negatively charged surface under the studied conditions, creating favorable electrostatic interactions with NH_4^+ cations (Figure 8). The proposed electrostatic mechanism for modified diatomite is supported by direct measurement of the zeta potential, confirming that at pH 7, above the pHpzc of all investigated sorbents (5.3–6.3), the alkaline treatment results in a stable negative surface charge necessary for ammonium cation capture.



Name	Mean	Minimum	Maximum
Z-Average (nm)	1078	1078	1078
Polydispersity Index (PI)	0.7448	0.7448	0.7448
Peak 1 Mean by Intensity ordered by area (nm)	2126	2126	2126
Peak 1 Area by Intensity ordered by area (%)	76.82	76.82	76.82
Peak 2 Mean by Intensity ordered by area (nm)	232.6	232.6	232.6
Peak 2 Area by Intensity ordered by area (%)	21.26	21.26	21.26

Name	Mean (d.nm)	Min (d.nm)	Max (d.nm)
Z-Average	1078	1078	1078
Polydispersity Index (PI)	0.7448	0.7448	0.7448
Peak 1 (Nano-fraction)	232.6	232.6	232.6
Peak 1 Area (Intensity)	21.26%	21.26	21.26
Peak 2 (Micro-fraction)	2126	2126	2126
Peak 2 Area (Intensity)	76.82%	76.82	76.82

Figure 8. Surface charge and colloidal behavior of modified diatomite in aqueous suspension: (**a**) ζ-potential and (**b**) dynamic light scattering (DLS) results.

Similar ζ-potential and DLS measurements were not performed for zeolite samples, as they did not exhibit significant dispersion in aqueous media and retained their stable granular structure. Therefore, the presented data reflect the behavior of diatomite specifically and do not imply direct mechanistic equivalence across all investigated materials.

The superior performance of modified diatomite may thus be attributed to the combined effects of its predominantly amorphous structure, enhanced dispersion behavior, and negative surface charge within the studied pH range. The high degree of fit to the PSO model (R^2 = 0.999) is not treated here as isolated proof of chemisorption, but rather as kinetic evidence that the rate-limiting step is governed by surface interactions. This interpretation is further justified by the convergence of multiple independent datasets: the thermodynamic agreement with the Langmuir model (R^2 = 0.999), indicating site-specific monolayer coverage; the electrochemical data (ζ potential of −29.75 mV), which provides a physical basis for strong electrostatic attraction of NH_4^+; and the spectroscopic shifts in FTIR, confirming the involvement of surface siloxane groups. Collectively, these results justify the conclusion that the process is a surface-controlled interaction involving strong electrostatic or chemical forces, rather than simple physical diffusion.

In practical wastewater treatment, the presence of competing cations such as Na^+, K^+, Mg^{2+}, and Ca^{2+} is an inevitable factor. Based on the ion-exchange and electrostatic mechanisms identified in this study, the adsorption of NH_4^+ is expected to be sensitive to the ionic strength of the solution. An increase in salt concentration can lead to the 'screening' of the negative surface charge of the modified diatomite, thereby reducing the attraction force for ammonium. While the current work utilized model solutions to isolate the effects of modification, future studies will evaluate the performance of these materials in multicomponent systems.

Overall, the data suggest distinct dominant mechanisms: ion exchange prevails in zeolite, whereas in modified diatomite, the combined improvement in textural properties (surface area) and surface characteristics (ζ-potential, dispersion behavior) enhances electrostatic attraction of NH_4^+ and leads to higher removal efficiency and q_{max} under the studied conditions.

FTIR after sorption (effect of contact with NH_4^+-N). After the interaction with the ammonium solution, a small additional shift in the main band (≈997 → ≈999 cm^{-1}) and a change in its intensity, as well as weak changes in the region of siloxane oscillations, are observed in the spectrum of the modified diatomite. These changes are small, but they are consistent with literature reports of surface silanol involvement in cation binding on amorphous silica [36,38], and may indicate the interaction of NH_4^+ with surface groups.

After sorption, the zeolite spectra show mainly intensity variations and local features in the range of ~1400–1430 cm^{-1}, while the position of the main frame bands remains almost unchanged.

In general, the observed spectral changes are moderate and interpreted cautiously, but they are consistent with the involvement of surface centers in the ammonium binding process. Experimental support for the interaction is further evidenced by post-sorption FTIR analysis, where moderate shifts in the siloxane region (≈997 → ≈999 cm^{-1}) suggest the redistribution of surface charge upon binding NH_4^+.

The proposed adsorption pathways are summarized in Figure 9 and suggest that NH_4^+ uptake proceeds through external mass transfer, intraparticle diffusion, and final surface interaction.

The proposed adsorption pathways are summarized in Figure 9 and suggest that NH_4^+ uptake proceeds through external mass transfer, intraparticle diffusion, and final surface interaction. Previous studies have shown that natural diatomite can retain ammonium in exchangeable and fixed forms, confirming the role of pore diffusion and surface

adsorption [14]. In addition, the porous silica structure and reactive surface groups of diatomite contribute to cation uptake [47]. For zeolite, enhanced NH_4^+ removal has been attributed to diffusion through internal channels and ion exchange with native cations after chemical treatment [48].

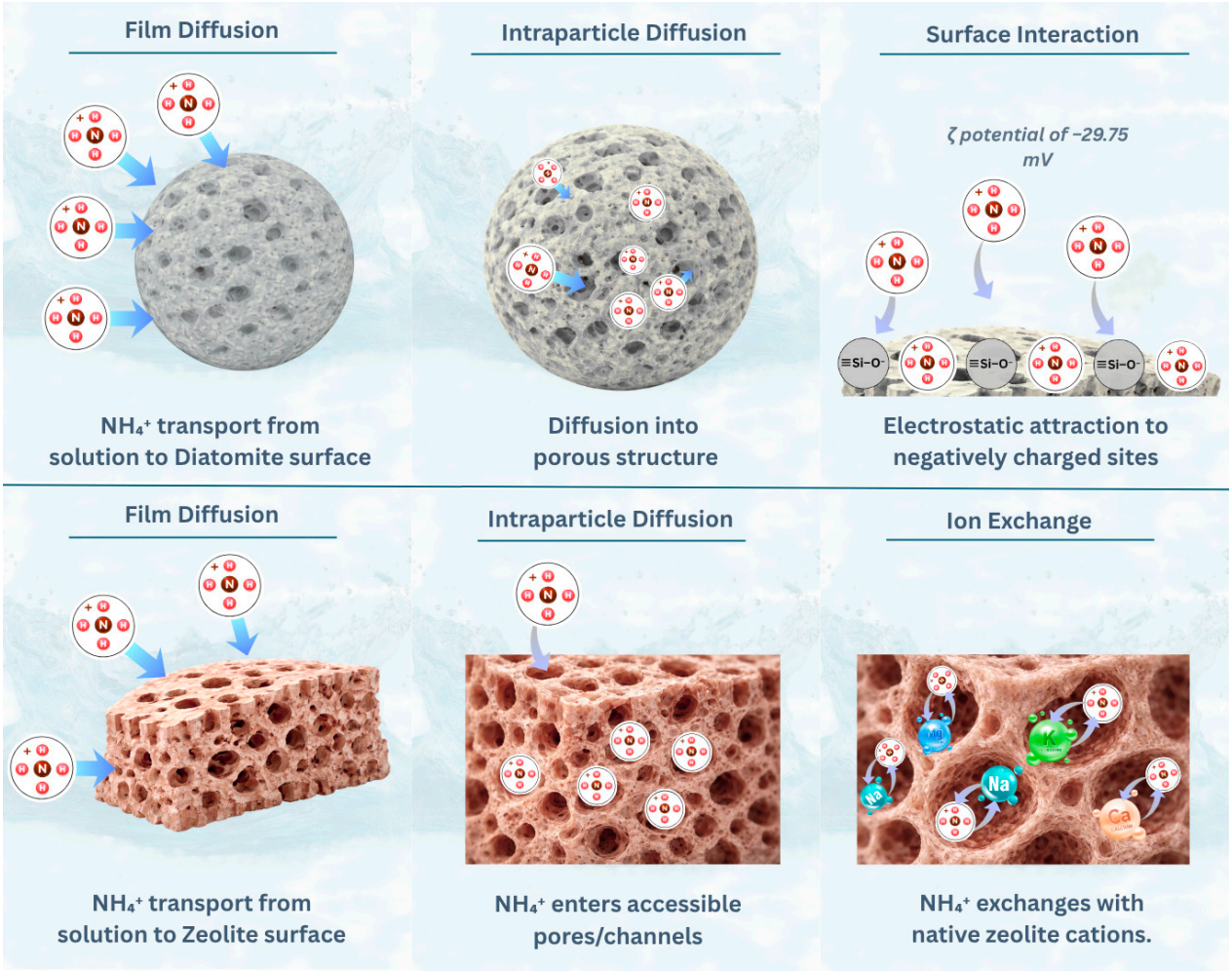


Figure 9. Schematic representation of the proposed NH_4^+ adsorption mechanisms for thermally and alkali-modified diatomite (**top row**) and zeolite (**bottom row**). For diatomite, NH_4^+ transport involves external film diffusion, intraparticle diffusion through the porous frustule network, and interaction with negatively charged surface sites (≡Si–O^-, ζ = −29.75 mV). For zeolite, the process includes film diffusion, diffusion through accessible channels and pores, and ion exchange with native cations (Na^+, K^+, Ca^{2+}, Mg^{2+}). The scheme is consistent with the kinetic and equilibrium results obtained in this study.

3.4.7. Comparison with Reported Adsorbents

To assess the competitiveness of the studied materials, their NH_4^+-N adsorption performance was compared with values reported in the literature for diatomite- and zeolite-based adsorbents under various modification conditions (Table 9).

The comparison presented in Table 9 shows that the modified diatomite used in this study achieved a q_{max} value of 1.758 mg/g and a removal efficiency of 84.6%, which is higher than those reported for some minimally modified diatomite-based systems, such as natural diatomite from PRB applications (0.677 mg/g) and functionalized diatomite treated with H_2SO_4/NaCl and calcination (0.716 mg/g). At the same time, the present values are lower than those obtained for more intensively engineered materials, including purified or oxide-composite diatomites and highly activated zeolites. Similar trends are

observed for the zeolite samples: the 0.5 M NaOH-modified zeolite in this work shows a moderate removal efficiency of about 70%, which places it in the general range of some pre-treated natural clinoptilolite systems, but remains below highly optimized zeolite materials reported in the literature.

Table 9. Comparison of NH_4^+-N adsorption performance of diatomite- and zeolite-based adsorbents reported in the literature with the results of the present study.

Adsorbent	Modification	q_{max} (mg/g)	Removal Efficiency (%)	Kinetic Model	Isotherm Model	Reference
Natural diatomite (PRB)	None	0.677	-	PFO	Langmuir	[14]
Functionalized diatomite (DTCA-Na)	H_2SO_4 + NaCl + calcination 400 °C	0.716	>80	PFO	Langmuir	[7]
Diatomite (DE)	None (Egyptian deposit)	63.16	97.2	PFO	Langmuir	[15]
Purified diatomite (PD)	Purification	-	69.5	-	Freundlich	[15]
Diatomite@MgO/CaO (D@MgO)	Metal oxide composite	78.3	100	PFO	Langmuir	[15]
Natural clinoptilolite	-	-	80	-	-	[48]
pre-treated clinoptilolite (NaOH)	1 M NaOH	-	83	-	-	[48]
pre-treated clinoptilolite (HCl)	0.1 M HCl	-	80	-	-	[48]
pre-treated clinoptilolite (NaOH-Na)	NaOH + 1 M NaCl	-	81	-	-	[48]
pre-treated clinoptilolite (NaOH-Ca)	NaOH + 0.5 M CaCl	-	83	-	-	[48]
pre-treated clinoptilolite (NaOH-Mg)	NaOH + 0.5 M MgCl	-	81	-	-	[48]
pre-treated clinoptilolite (HCl-Na)	HCl + 1 M NaCl	-	79	-	-	[48]
pre-treated clinoptilolite (HCl-Ca)	HCl + 0.5 M CaCl	-	76	-	-	[48]
pre-treated clinoptilolite (HCl-Mg)	HCl + 0.5 M MgCl	-	79	-	-	[48]
NaCl-modified zeolite (M-Zeo)	NaCl treatment	-	-	PSO	Freundlich	[12]
HCl-modified clinoptilolite (HZU2)	Ultrasonic + HCl	142.85	≥99	PSO	Langmuir	[49]
Natural clinoptilolite (Lee et al.)	Thermal 0–900 °C	-	78.5 (natural) → 1.4% (900 °C)	PSO	Freundlich	[25]
Foundry dust NaA zeolite (FZA)	Synthesis from waste	37.81	95	PSO	Langmuir	[50]
Natural diatomite (this study)	-	-	~46	PSO	Freundlich	This study
Modified diatomite (this study)	Thermal 450 °C + 0.5 M NaOH	1.758	84.6	PSO	Langmuir	This study
Natural zeolite (this study)	-	-	~53	PSO	Freundlich	This study
Modified zeolite (this study)	0.5 M NaOH	-	~70	PSO	Freundlich	This study

These differences should be interpreted with caution, because the literature values summarized in Table 9 are not strictly comparable unless the experimental conditions are similar and the same performance metric is reported. In particular, q_{max} values depend strongly on initial concentration range, pH, contact time, solution chemistry, and the extent of material functionalization. Many of the higher-performing literature examples involve stronger acid/alkali treatment, ultrasonic assistance, or composite formation with metal oxides, which substantially increase the number of available active sites and can produce much larger capacities than those expected for a mild thermal–alkaline treatment. In contrast, the present work was intentionally designed to preserve the natural structure of the minerals while using a simple and low-cost modification route. Therefore, the obtained capacities should be viewed as a realistic performance benchmark for locally available sorbents rather than as an absolute upper limit of ammonium uptake.

From this perspective, the main contribution of the present study is not the demonstration of the highest possible capacity, but rather the identification of a simple activation strategy that significantly improves the performance of natural diatomite while keeping the treatment conditions mild and technically feasible. This is particularly important for practical wastewater treatment, where cost, reagent consumption, and structural stability are often as important as maximum adsorption capacity.

3.4.8. Regeneration and Reusability

To assess the practical suitability of sorbents for reuse, five consecutive adsorption–desorption cycles were performed under identical conditions (Figure 10). After each cycle, the efficiency of NH_4^+-N removal was evaluated repeatedly using regenerated materials. All sorbents retained measurable adsorption activity for five cycles, although the degree of loss of characteristics was different for different samples.

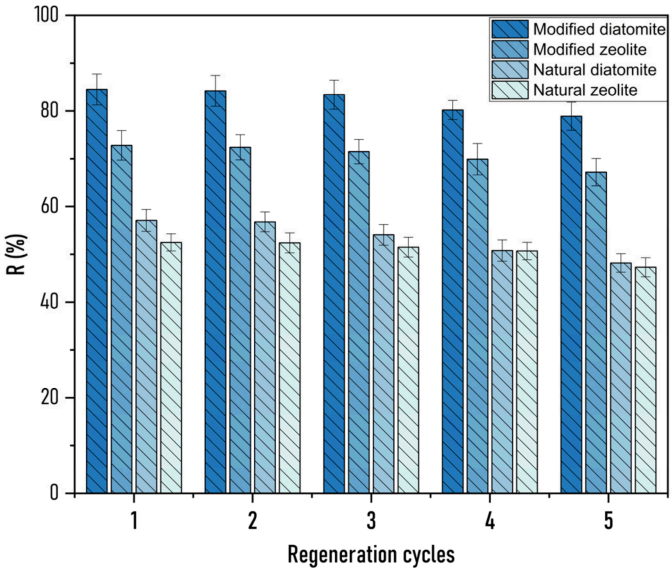


Figure 10. NH_4^+-N removal efficiency (R, %) of natural and modified diatomite and zeolite over five consecutive adsorption–desorption cycles.

The modified diatomite demonstrated the best stability, decreasing from 84.56% in the first cycle to 78.9% in the fifth cycle, which corresponds to maintaining approximately 93.4% of its original effectiveness. This result is consistent with the findings of Fang et al. [7], who reported that functionalized diatomite retained above 80% NH_4^+-N removal efficiency after five adsorption–desorption cycles, confirming that chemical and thermal surface activation improves the reversibility of ammonium uptake. Modified zeolite showed a similar trend,

decreasing from 72.8% to 67.2% (retention 92.3%), which is in agreement with Pan et al. [12], who observed a regeneration rate of 90.6% after five cycles for NaCl-modified zeolite.

Natural materials showed a more pronounced decrease, especially natural diatomite, whose efficiency decreased from 57.1% to 48.2% (retention 84.4%). This stronger degradation of unmodified diatomite is consistent with previous reports [14], which showed that a considerable portion of NH_4^+ adsorbed on natural diatomite becomes chemically fixed and is therefore not easily removed during regeneration. As a result, the number of available adsorption sites gradually decreases over repeated cycles. Natural zeolite decreased from 52.5% to 47.3% (retention 90.1%), which is consistent with previously reported values for clinoptilolite regenerated with NaCl under alkaline conditions [51]. These results indicate a gradual rather than abrupt loss of capacity during repeated salt regeneration.

A gradual rather than drastic decrease in productivity suggests a partial recovery of adsorption capacity after regeneration, but the results presented should be interpreted with caution, since the desorption efficiency has not been quantified separately. Therefore, the observed decrease may reflect both incomplete removal of previously adsorbed NH_4^+—a limitation previously noted for NaCl-based protocols, which typically recover only a fraction of sorbed ammonium per cycle [50] and progressive deactivation of available surface areas. Among the materials studied, modified diatomite and modified zeolite demonstrated the most stable short-term recyclability, which indicates that pre-heat treatment followed by weak alkaline activation improves not only the initial adsorption performance, but also the resistance to loss of characteristics during reuse.

3.5. Limitations and Future Work

The present study was designed to evaluate the intrinsic adsorption behavior of thermally and alkali-modified diatomite and zeolite under controlled laboratory conditions. For this reason, model NH_4^+-N solutions were used instead of real wastewater. This approach allowed us to isolate the effect of sorbent modification and to compare the materials under identical and reproducible conditions. In real wastewater treatment, performance may be influenced by competing ions, dissolved organic matter, suspended solids, and hydraulic conditions. Therefore, the present study should be considered a screening and mechanistic investigation, while column operation, and multicomponent validation are required before practical implementation.

Another limitation of the present study is the absence of a thermodynamic analysis. Such an analysis requires equilibrium data obtained at multiple temperatures and is therefore outside the scope of the current experimental design, which was focused on the optimization of sorbent modification and the evaluation of adsorption behavior at room temperature, the condition most relevant to practical wastewater treatment in the studied region. Nevertheless, the pH-dependence, kinetic fitting, and ζ-potential data provide a consistent physical basis for interpreting the adsorption mechanism. Future work will therefore focus on validation in real wastewater, multicomponent systems, regeneration performance, continuous-flow tests, and temperature-dependent thermodynamic characterization.

4. Conclusions

This study showed that diatomite and zeolite from Kazakhstan deposits can be used for ammonium nitrogen removal after mild thermal and alkaline modification, although their response to treatment and dominant adsorption pathways were not the same. For diatomite, calcination at 450 °C followed by treatment with 0.5 M NaOH gave the most favorable combination of textural development and structural stability: the specific surface area increased to 46.32 m^2/g, the total pore volume reached 0.179 cm^3/g, and the pore structure was dominated by mesopores (V_{meso} = 0.164 cm^3/g, >93% of total porosity). XRD

and FTIR showed that these changes occurred without noticeable rearrangement of the siliceous framework.

The modified diatomite showed the best adsorption performance among the investigated materials, with 84.6% NH_4^+-N removal and a Langmuir q_{max} of 1.758 mg/g. Its adsorption kinetics were best described by the pseudo-second-order model (R^2 = 0.999, h = 0.0166 mg/g·min), while the equilibrium data were fitted most closely by the Langmuir model, indicating favorable monolayer adsorption under the studied conditions. The separation factor R_L ranged from 0.068 to 0.643 across all materials, confirming favorable adsorption in the tested concentration range. The pHpzc values of the investigated sorbents ranged from 5.3 to 6.3, and at pH 7, all surfaces carried a negative charge, which supports the electrostatic attraction of NH_4^+ cations. For the modified diatomite, the measured ζ-potential of −29.75 mV further supports this interpretation.

In contrast, zeolite retained its crystalline aluminosilicate framework after 0.5 M NaOH treatment but showed more moderate textural and adsorption changes (q_{max} = 0.741 mg/g for modified zeolite versus 0.532 mg/g for natural zeolite). Its behavior was mainly governed by cation exchange within the structural channels, whereas modified diatomite was controlled largely by surface adsorption on a more accessible mesoporous and hydroxyl-rich surface. The regeneration tests also showed that the modified materials were more stable than their natural counterparts over repeated use: modified diatomite retained 93.4% of its initial removal efficiency after five cycles (84.56 → 78.9%), and modified zeolite retained 92.3% (72.8 → 67.2%), compared with 84.4% and 90.1% for the corresponding natural forms. This indicates that the proposed modification strategy improves not only the initial performance but also the resistance to capacity loss during reuse.

At the same time, the present study was carried out under controlled model-solution conditions at ambient temperature, which limits direct extrapolation to real wastewater treatment. Validation under multicomponent conditions, assessment of competitive ion effects, longer regeneration cycling beyond five runs, and temperature-dependent thermodynamic analysis remain important tasks for future work. Overall, the results show that simple thermal–alkaline activation can convert naturally abundant and locally available mineral sorbents into useful materials for ammonium removal, with particular relevance for decentralized and resource-constrained treatment systems in regions where access to advanced infrastructure is limited.

Supplementary Materials: The following supporting information can be downloaded at: https://www.mdpi.com/article/10.3390/w18091104/s1, Figure S1: Nitrogen adsorption-desorption isotherms of natural zeolite (NZ), modified zeolite (MZ), natural diatomite after calcination (ND), and modified diatomite (MD). Adsorption branches (ads) are represented by filled square symbols; desorption branches (des) are represented by filled circle symbols; Table S1: Diatomite; Table S2: Zeolite.

Author Contributions: Conceptualization, G.B., M.A. and Y.D.; methodology, G.B., M.A., Y.D., O.D. and B.I.; software, L.K.; validation, D.B. and U.M.; investigation, G.B., L.K., A.Z. and D.B.; formal analysis, A.Z. and D.A.; data curation, G.B., D.A., D.B. and U.M.; writing—original draft preparation, G.B., Y.D. and A.Z.; writing—review and editing, W.P., G.B., L.K., O.D., B.I. and U.M.; visualization, G.B., D.A., U.M. and M.A.; resources, O.D., B.I., D.B. and Y.D.; supervision, M.A., W.P., Y.D. and O.D.; project administration, Y.D.; funding acquisition, Y.D. All authors have read and agreed to the published version of the manuscript.

Funding: This work was supported by the Ministry of Science and Higher Education of the Republic of Kazakhstan grant (AP23489070).

Data Availability Statement: The original contributions presented in this study are included in the article. Further inquiries can be directed to the corresponding author.

Conflicts of Interest: The authors declare no conflicts of interest.

Abbreviations

The following abbreviations are used in this manuscript:

PFO	Pseudo-first-order
PSO	Pseudo-second-order
DLS	Dynamic light scattering

References

1. Schindler, D.W. Recent advances in the understanding and management of eutrophication. *Limnol. Oceanogr.* **2006**, *51*, 356–363. [CrossRef]
2. Dorgham, M.M. Effects of eutrophication. In *Eutrophication: Causes, Consequences and Control*; Springer: Dordrecht, The Netherlands, 2013; Volume 2, pp. 29–44. [CrossRef]
3. Sabitov, A.; Ibragimova, N.; Lyu, M.; Bolatova, D. About the need for developing risk management for ensuring safety from antibiotic and veterinary drug residues in Kazakhstan. *J. Sustain. Sci. Manag.* **2021**, *16*, 303–315. [CrossRef]
4. Han, B.; Butterly, C.; Zhang, W.; He, J.Z.; Chen, D. Adsorbent materials for ammonium and ammonia removal: A review. *J. Clean. Prod.* **2021**, *283*, 124611. [CrossRef]
5. Alshameri, A.; He, H.; Zhu, J.; Xi, Y.; Zhu, R.; Ma, L.; Tao, Q. Adsorption of ammonium by different natural clay minerals: Characterization, kinetics and adsorption isotherms. *Appl. Clay Sci.* **2018**, *159*, 83–93. [CrossRef]
6. Wang, X.; Lü, S.; Gao, C.; Feng, C.; Xu, X.; Bai, X.; Gao, N.; Yang, J.; Liu, M.; Wu, L. Recovery of ammonium and phosphate from wastewater by wheat straw-based amphoteric adsorbent and reusing as a multifunctional slow-release compound fertilizer. *ACS Sustain. Chem. Eng.* **2016**, *4*, 2068–2079. [CrossRef]
7. Fang, S.; Li, G.; Shi, H.; Ye, J.; Wang, H.; Ding, X.; Luo, L.; Li, G.; Yang, M. Preparation of low-cost functionalized diatomite and its effective removal of ammonia nitrogen from wastewater. *Environ. Sci. Pollut. Res.* **2023**, *30*, 98881–98894. [CrossRef] [PubMed]
8. Grela, A.; Łach, M.; Pamuła, J.; Łach, K.; Godyń, I.; Malina, D.; Wzorek, Z.; Setlak, K.; Grela, D. Effect of diatomite application on the removal of biogenic pollutants in rain gardens. *Materials* **2024**, *17*, 6279. [CrossRef] [PubMed]
9. Yadav, V.; Rani, M.; Kumar, L.; Singh, N.; Ezhilselvi, V. Effect of surface modification of natural zeolite on ammonium ion removal from water using batch study: An overview. *Water Air Soil Pollut.* **2022**, *233*, 465. [CrossRef]
10. Taddeo, R.; Prajapati, S.; Lepistö, R. Optimizing ammonium adsorption on natural zeolite for wastewaters with high loads of ammonium and solids. *J. Porous Mater.* **2017**, *24*, 1545–1554. [CrossRef]
11. Ivanova, E.; Karsheva, M.; Koumanova, B. Adsorption of ammonium ions onto natural zeolite. *J. Univ. Chem. Technol. Metall.* **2010**, *45*, 295–302.
12. Pan, M.; Zhang, M.; Zou, X.; Zhao, X.; Deng, T.; Chen, T.; Huang, X. The investigation into the adsorption removal of ammonium by natural and modified zeolites: Kinetics, isotherms, and thermodynamics. *Water SA* **2019**, *45*, 648–656. [CrossRef]
13. Ates, A. Effect of alkali-treatment on the characteristics of natural zeolites with different compositions. *J. Colloid Interface Sci.* **2018**, *523*, 266–281. [CrossRef] [PubMed]
14. Zhou, Y.; Chen, L.; Wang, J.; Lu, L.; Liu, F.; Chen, C.; Qin, X. Solution, exchangeable and fixed ammonium in natural diatomite as a simulated PRB material: Effects of adsorption and bioregeneration processes. *Environ. Sci. Pollut. Res.* **2023**, *30*, 52433–52445. [CrossRef]
15. AbuKhadra, M.R.; Eid, M.H.; Allam, A.A.; Ajarem, J.S.; Almalki, A.M.; Salama, Y. Evaluation of different forms of Egyptian diatomite for the removal of ammonium ions from Lake Qarun: A realistic study to avoid eutrophication. *Environ. Pollut.* **2020**, *266*, 115277. [CrossRef]
16. Chen, H.-F.; Lin, Y.-J.; Chen, B.-H.; Yoshiyuki, I.; Liou, S.Y.-H.; Huang, R.-T. A further investigation of NH4+ removal mechanisms by using natural and synthetic zeolites in different concentrations and temperatures. *Minerals* **2018**, *8*, 499. [CrossRef]
17. Widiastuti, N.; Wu, H.; Ang, H.M.; Zhang, D. Removal of ammonium from greywater using natural zeolite. *Desalination* **2011**, *277*, 15–23. [CrossRef]
18. Zhao, Y.P.; Gao, T.Y.; Jiang, S.Y.; Cao, D.W. Ammonium removal by modified zeolite from municipal wastewater. *J. Environ. Sci.* **2004**, *16*, 1001–1004.
19. Canellas-Garriga, J. Tertiary Ammonium Removal with Zeolites. Doctoral Dissertation, Cranfield University, Cranfield, UK, 2018. Available online: https://dspace.lib.cranfield.ac.uk/handle/1826/18386 (accessed on 22 February 2026).
20. Das, D.; Sengupta, S. Modified zeolite in a sustainable, circular economy-based process for enhanced ammonium recovery from wastewater. *Clean. Water* **2025**, *3*, 100075. [CrossRef]
21. Zhou, H.D.; Wang, C.Y.; Wang, Q.; Xu, B.X.; Zhu, G. Efficiency, mechanism and application prospect of ammonium adsorption and desorption over a sodium-acetate-modified synthetic zeolite. *RSC Adv.* **2024**, *14*, 17843–17854. [CrossRef]
22. Tsai, W.T.; Hsien, K.J.; Lai, C.W. Chemical activation of spent diatomaceous earth by alkaline etching in the preparation of mesoporous adsorbents. *Ind. Eng. Chem. Res.* **2004**, *43*, 7513–7520. [CrossRef]

23. Yann, T.; Winotapun, C.; Yos, P.; Voon, L.H.; Boondamnoen, O. Particle characteristics of diatomite activated by alkaline solution. *Adv. Sci. Technol.* **2024**, *155*, 37–43. Available online: https://www.scientific.net/AST.155.37 (accessed on 22 February 2026). [CrossRef]
24. Zhao, Y.H.; Geng, J.T.; Cai, J.C.; Cai, Y.F.; Cao, C.Y. Adsorption performance of basic fuchsin on alkali-activated diatomite. *Adsorpt. Sci. Technol.* **2020**, *38*, 151–167. [CrossRef]
25. Lee, J.I.; Lee, C.G.; Hong, S.C.; Park, S.G. Multifunctional application of zeolite for ammonium removal and ammonia emission mitigation in wastewater, carcass leachate, and paddy. *Sci. Rep.* **2026**, *16*, 6327. [CrossRef]
26. International Centre for Diffraction Data (ICDD). Available online: https://www.icdd.com/ (accessed on 4 March 2026).
27. Tran, H.N.; You, S.J.; Hosseini-Bandegharaei, A.; Chao, H.P. Mistakes and inconsistencies regarding adsorption of contaminants from aqueous solutions: A critical review. *Water Res.* **2017**, *120*, 88–116. [CrossRef]
28. Wang, J.; Guo, X. Adsorption kinetic models: Physical meanings, applications, and solving methods. *J. Hazard. Mater.* **2020**, *390*, 122156. [CrossRef] [PubMed]
29. Wang, J.; Guo, X. Adsorption isotherm models: Classification, physical meaning, application and solving method. *Chemosphere* **2020**, *258*, 127279. [CrossRef]
30. Khan, M.N.; Sarwar, A. Determination of points of zero charge of natural and treated adsorbents. *Surf. Rev. Lett.* **2007**, *14*, 461–469. [CrossRef]
31. Kuldeyev, E.; Seitzhanova, M.; Tanirbergenova, S.; Tazhu, K.; Doszhanov, E.; Mansurov, Z.; Azat, S.; Nurlybaev, R.; Berndtsson, R. Modifying natural zeolites to improve heavy metal adsorption. *Water* **2023**, *15*, 2215. [CrossRef]
32. Akhmetzhanova, D.; Sabitov, A.; Doszhanov, Y.; Atamanov, M.; Saurykova, K.; Zhumazhanov, A.; Atamanova, T.; Kerimkulova, A.; Velasco, L.F.; Zhumagalieva, A.; et al. Zeolites and activated carbons in hydroponics: A systematic review of mechanisms, performance metrics, techno-economic analysis and life-cycle assessment. *Sustainability* **2025**, *17*, 10977. [CrossRef]
33. Zahid, M.; Doszhanov, Y.; Saurykova, K.; Ahmadi, N.; Bolatova, D.; Kurmanbayeva, M.; Aydarbek, A.; Ihsas, R.; Seitzhanova, M.; Akhmetzhanova, D.; et al. Modification and Application of Natural Clinoptilolite and Mordenite from Almaty Region for Drinking Water Purification. *Molecules* **2025**, *30*, 2021. [CrossRef] [PubMed]
34. Doszhanov, Y.; Akhmetzhanova, D.; Fernandez Velasco, L.; Khamitova, K.; Zhumazhanov, A.; Arifzade, E.; Saurykova, K.; Sabitov, A.; Mansurov, Z.; Atamanov, M.; et al. Impact of Zeolites on Growth Dynamics of Medicago sativa and Lactuca sativa in Hydroponics. *Plants* **2026**, *15*, 736. [CrossRef]
35. Antosik, A.K.; Mozelewska, K.; Musik, M.; Miądlicki, P. Influence of diatomite and its base modifications on the self-adhesive properties of silicone pressure-sensitive adhesives. *Sci. Rep.* **2023**, *13*, 13691. [CrossRef]
36. Ellerbrock, R.; Stein, M.; Schaller, J. Comparing amorphous silica, short-range-ordered silicates and silicic acid species by FTIR. *Sci. Rep.* **2022**, *12*, 11708. [CrossRef]
37. Aguedal, H.; Iddou, A.; Aziz, A.; Shishkin, A.; Ločs, J.; Juhna, T. Effect of thermal regeneration of diatomite adsorbent on its efficacy for removal of dye from water. *Int. J. Environ. Sci. Technol.* **2019**, *16*, 113–124. [CrossRef]
38. Carotenuto, G. Water Physisorbed on Natural Clinoptilolite. Encyclopedia 2020. Available online: https://encyclopedia.pub/entry/1243 (accessed on 17 April 2026).
39. Yuan, P.; Wu, D.Q.; He, H.P.; Lin, Z.Y. The hydroxyl species and acid sites on diatomite surface: A combined IR and Raman study. *Appl. Surf. Sci.* **2004**, *227*, 30–39. [CrossRef]
40. Jiao, J.L.; Yang, S.W.; Xie, Y.; Jin, W.D.; Yan, Y.H.; Xu, B. Adsorption properties of ammonia nitrogen in aqueous solution by various materials. *Huanjing Kexue* **2019**, *40*, 3633–3641. [PubMed]
41. Sarioglu, M. Removal of ammonium from municipal wastewater using natural Turkish (Dogantepe) zeolite. *Sep. Purif. Technol.* **2005**, *41*, 1–11. [CrossRef]
42. Karadag, D.; Koc, Y.; Turan, M.; Ozturk, M. A comparative study of linear and non-linear regression analysis for ammonium exchange by clinoptilolite zeolite. *J. Hazard. Mater.* **2007**, *144*, 432–437. [CrossRef]
43. Kučić, D.; Čosić, I.; Vuković, M.; Briški, F. Sorption kinetic studies of ammonium from aqueous solution on different inorganic and organic media. *Acta Chim. Slov.* **2013**, *60*, 109. [PubMed]
44. Xu, H.; Wang, B.; Zhao, R.; Wang, X.; Pan, C.; Jiang, Y.; Ge, B. Adsorption behavior and performance of ammonium onto sorghum straw biochar from water. *Sci. Rep.* **2022**, *12*, 5358. [CrossRef]
45. Eberle, S.; Börnick, H.; Stolte, S. Granular Natural Zeolites: Cost-Effective Adsorbents for the Removal of Ammonium from Drinking Water. *Water* **2022**, *14*, 939. [CrossRef]
46. Adam, M.R.; Othman, M.H.D.; Hubadillah, S.K.; Abd Aziz, M.H.; Jamalludin, M.R. Application of natural zeolite clinoptilolite for the removal of ammonia in wastewater. *Mater. Today Proc.* **2023**, *64*, 317–323. [CrossRef]
47. Zhao, Y.; Tian, G.; Duan, X.; Liang, X.; Meng, J.; Liang, J. Environmental applications of diatomite minerals in removing heavy metals from water. *Ind. Eng. Chem. Res.* **2019**, *58*, 11638–11652. [CrossRef]
48. Muscarella, S.M.; Badalucco, L.; Cano, B.; Laudicina, V.A.; Mannina, G. Ammonium adsorption, desorption and recovery by acid and alkaline treated zeolite. *Bioresour. Technol.* **2021**, *341*, 125812. [CrossRef] [PubMed]

49. Jahani, F.; Sadeghi, R.; Shakeri, M. Ultrasonic-assisted chemical modification of a natural clinoptilolite zeolite: Enhanced ammonium adsorption rate and resistance to disturbing ions. *J. Environ. Chem. Eng.* **2023**, *11*, 110354. [CrossRef]
50. Wang, M.; Xu, D.; Ma, H.; Li, B.; Howard, A. Synthesis of NaA zeolite from foundry dust and its adsorption capacity of ammonia. *J. Environ. Manag.* **2023**, *331*, 117297. [CrossRef]
51. Castro, C.J.; Shyu, H.Y.; Xaba, L.; Bair, R.; Yeh, D.H. Performance and onsite regeneration of natural zeolite for ammonium removal in a field-scale non-sewered sanitation system. *Sci. Total Environ.* **2021**, *776*, 145938. [CrossRef]

Disclaimer/Publisher's Note: The statements, opinions and data contained in all publications are solely those of the individual author(s) and contributor(s) and not of MDPI and/or the editor(s). MDPI and/or the editor(s) disclaim responsibility for any injury to people or property resulting from any ideas, methods, instructions or products referred to in the content.